I. MEASUREMENT OF THE LATENT HEAT OF VAPORIZATION OF LIGHTER HYDROCARBONS--VALUES FOR NORMAL OCTANE

II. VOLUMETRIC AND PHASE BEHAVIOR IN THE ETHANE-PROPENE SYSTEM

Thesis by

Richard Alan McKay

In Partial Fulfillment of the Requirements

For the Degree of

Doctor of Philosophy

California Institute of Technology

Pasadena, California

1959

ACKNOWLEDGMENT

Many people contributed assistance both directly and indirectly during the course of this work. In particular I wish to express my appreciation to Professor Bruce H. Sage for his patient guidance and helpful advice. Much of the success of this work is due to the direction and cooperation which he provided. The cooperation of H. Hollis Reamer is also appreciated. The contributions of Willard M. Dewitt, George A. Griffith, Seichi Nakawatase, Jean Garcin, Torvald Myklebust, Paul B. Holmen, Lee T. Carmichael, Henry E. Smith and others are gratefully acknowledged. The assistance of William Kozicki during the course of the investigation is also gratefully acknowledged. The suggestions of Professors William N. Lacey, Paul A. Longwell, and William H. Corcoran each of whom reviewed the manuscript, are appreciated. The typing was done by Alethea Miller.

I wish to acknowledge with gratitude the financial assistance of California Research Corporation during the four years covered by this work. Much of the apparatus used in this investigation was made available by the Jet Propulsion Laboratory.

ABSTRACT

I. A calorimeter, originally built to measure the heat capacities of liquids at temperatures from 100 to 400°F and at pressures up to 1000 pounds per square inch, was modified to extend its utility to include the measurement of latent heats of vaporization of liquids over the same range of conditions. A description of the apparatus and of the procedure used for determining experimentally the heat of vaporization is presented in detail.

Experimentally determined values of the latent heat of vaporization of n-octane at temperatures from 100 to 340°F are presented. The results at the lower temperatures agree with the measurements of the National Bureau of Standards within 0.09 per cent. At the higher temperatures the results are within 2 per cent of the values calculated from volumetric and phase behavior data.

II. The molal volumes of three mixtures of ethane and propene were measured at pressures up to 10,000 pounds per square inch in the temperature interval between 10 and 400°F. The compositions of the coexisting phases were established throughout the two-phase region of this system at temperatures from 10 to 160°F.

TABLE OF CONTENTS

PART I

MEASUREMENT OF THE LATENT HEAT OF VAPORIZATION OF LIGHTER HYDROCARBONS--VALUES FOR NORMAL OCTANE

INTRODUCTION

The latent heat of vaporization is of importance in establishing the thermodynamic behavior of pure substances in the two-phase region of saturated liquid and gas. Although this quantity may be calculated from volumetric and vapor pressure data by means of the Clapeyron equation, it can be determined more accurately in certain regions by direct measurement. Among the available values of the latent heat of vaporization, experimental data are a small minority, and most of these represent determinations at atmospheric pressure or lower. The object of the present work has been to adapt to vaporization studies a calorimeter (1) which was originally built for the measurement of the heat capacities of liquids, and to carry out measurements of the latent heat of vaporization of n-octane at temperatures from 100 to 340°F.

n-Heptane was recommended by the Fourth Conference on Low Temperature Calorimetry (2) as a suitable material for use in the intercomparison of precision calorimeters. In order to check the general operation of the modified apparatus, the latent heat of vaporization of n-heptane was measured at 100°F.

Latent heat of vaporization values for n-heptane have been determined by several investigators from measurements of the weight of n-heptane evolved from a calorimeter as a result of the addition of a known quantity of electrical energy. Osborne and Ginnings (3) carried out such measurements near room temperature. Measurements near the normal boiling point (209.2°F) were made by Pitzer (4) and by Mathews (5), and a value at the normal boiling point was reported by Rossini (6). Determinations at intermediate temperatures were made by Waddington and coworkers (7). By means of the Clapeyron equation, Young (8) calculated the latent heat of vaporization of n-heptane in the range from 158°F to the critical temperature (512.3°F) from his measurements of the vapor pressure and the specific volume of the saturated liquid and the saturated gas as functions of temperature. The data reported by Osborne and Ginnings (3), Waddington and coworkers (7), and some of the calculated values reported by Young (8) are in good agreement.

Latent heats of vaporization of n-octane have also been reported. Osborne and Ginnings (3) carried out measurements at 77°F. A value at the normal boiling point (258.2°F) was reported by Rossini (6) and values near the normal boiling point and at one lower temperature were measured by Barrow (9). Young calculated the latent heat of vaporization of n-octane at temperatures from 248°F to the critical temperature (565.2°F) from pressure-volume-temperature measurements. In the temperature region where direct comparison is possible, these data are in agreement to within approximately 3 per cent.

METHOD AND APPARATUS

The method used and the general features of the apparatus were essentially the same as developed by Osborne and coworkers (3,10,11). In principle, the method consisted of adding a known amount of electrical energy to an isochoric calorimeter containing liquid and gas phases of the substance being studied, and determining the weight of material withdrawn as saturated gas, while maintaining a constant temperature and pressure within the calorimeter.

The general features of the calorimeter and associated equipment are shown schematically in Figure 1. The calorimeter A was mounted within a vacuum jacket B which was surrounded by an oil bath, not shown. A small centrifugal agitator C served to circulate the liquid in the calorimeter past a heater D, around and through a shield E, and past a thermometer well F. Provision was made for measuring the pressure with a pressure balance G through a connection at the bottom of the calorimeter. The saturated gas was withdrawn through a small tube H at a rate controlled by a small orifice meter I. The orifice was operated under conditions of critical flow (viz., pressure ratio greater than 2:1 across the orifice) so that the rate of flow was insensitive to minor variations in pressure downstream from the orifice but was dependent upon the pressure in the calorimeter. The withdrawn sample was condensed in either of two weighing bombs J and K. Condensation in the withdrawal tube was prevented by maintaining this part of the apparatus at a temperature slightly above that of the calorimeter. The wall of the vacuum jacket B and the calorimeter A were held at substantially the same temperature to prevent any significant exchange of energy between the calorimeter and the jacket. The pressure within the vacuum jacket was maintained below 10^{-8} inches of mercury by means of an oil diffusion pump L and a suitable mechanical forepump.

THERMODYNAMIC ANALYSIS

For a system which undergoes a process involving heat, work, and change in weight, the first law of thermodynamics states that*

$$d\underline{E} = q - \underline{w} + E' dm \tag{1}$$

In this analysis it is assumed that the material is withdrawn as gas at the state in which it exists within the calorimeter. Therefore

$$E' = E_g \tag{2}$$

The term q represents the net transfer of energy to the system and includes the energy transmitted electrically, energy introduced by means of the agitator, and thermal transfer by conduction and radiation. That is

$$q = q_e + q_s + q_J \tag{3}$$

Since the calorimeter is isochoric, the work term is concerned only with the work associated with the withdrawal

---

*Symbols which are used in the text are defined in the nomenclature which follows the references.

of material, so that

$$\underline{\omega} = -PV_g\,dm \tag{4}$$

The change in the total internal energy of the system including the calorimeter may be expressed as the sum of the changes in the total internal energy of both phases and of the calorimeter:

$$d\underline{E} = d\underline{E}_g + d\underline{E}_\ell + d\underline{E}_A \tag{5}$$

The total internal energy of the gas phase is given by

$$\underline{E}_g = m_g E_g \tag{6}$$

Equation 6 may be differentiated to give the change in total internal energy of the gas phase:

$$d\underline{E}_g = m_g\,dE_g + E_g\,dm_g \tag{7}$$

Similarly the change in total internal energy of the liquid phase is

$$d\underline{E}_\ell = m_\ell\,dE_\ell + E_\ell\,dm_\ell \tag{8}$$

If Equations 7 and 8 are combined with Equation 5, the change in the total internal energy of the system may be written as

$$d\underline{E} = E_g\,dm_g + E_\ell\,dm_\ell + m_g\,dE_g + m_\ell\,dE_\ell + d\underline{E}_A \quad (9)$$

By substituting Equations 2, 3 and 4 in Equation 1 and combining with Equation 9 there results

$$E_g\,dm_g + E_\ell\,dm_\ell + \left[m_g\,dE_g + m_\ell\,dE_\ell + d\underline{E}_A\right] = q + PV_g\,dm - E_g\,dm \quad (10)$$

In the foregoing analysis, it has been assumed that each of the phases may be represented by a single state although in an actual situation temperature gradients occur within each phase. Except for this assumption, equation 10 is rigorous.

Ideally, the vaporization process is carried out isothermally, whereas in practice, small variations in state are usually encountered with respect to time as well as position. The effect of variation with respect to time is important and is indicated in Equation 10 and in the succeeding equations by the bracketed terms. The effect of variation with respect to position within each phase is negligible and has been omitted from the treatment.

The total weight of material within the system may be represented by

$$m = m_g + m_\ell \tag{11}$$

If Equation 11 is differentiated, there results

$$dm = dm_g + dm_\ell \tag{12}$$

Substitution for dm_g in the first term of Equation 10 and for dm in the work term, $PV_g dm$, gives

$$-dm_\ell(E_g - E_\ell) + \left[m_g dE_g + m_\ell dE_\ell + d\underline{E}_A\right] = q + PV_g dm_g + PV_g dm_\ell \tag{13}$$

The total volume of the system is given by

$$\underline{V} = \underline{V}_g + \underline{V}_\ell = m_g V_g + m_\ell V_\ell \tag{14}$$

Differentiation of Equation 14, recalling that the calorimeter is isochoric, gives

$$0 = V_g dm_g + V_\ell dm_\ell + \left[m_g dV_g + m_\ell dV_\ell\right] \tag{15}$$

Combination of Equations 13 and 15 results in

$$-dm_\ell\left(E_g - E_\ell\right) + \left[m_g\, dE_g + m_\ell\, dE_\ell + d\,\underline{E}_A\right] \qquad (16)$$
$$= q - PV_\ell\, dm_\ell + PV_g\, dm_\ell - P\left[m_g\, dV_g + m_\ell\, dV_\ell\right]$$

Rearrangement of Equation 16 and substitution of the enthalpy, $H\,'$, for the $(E + PV)$ terms resulting, yields

$$-dm_\ell\left(H_g - H_\ell\right) = q - m_g\left[dE_g + P\,dV_g\right] - m_\ell\left[dE_\ell + P\,dV_\ell\right] - \left[d\,\underline{E}_A\right] \qquad (17)$$

Eliminating dm_g from Equation 15 by means of Equation 12, the change in weight of the liquid phase is related to the weight of material withdrawn from the system by

$$dm_\ell = \frac{V_g}{V_g - V_\ell}\, dm + \frac{\left[m_g\, dV_g + m_\ell\, dV_\ell\right]}{V_g - V_\ell} \qquad (18)$$

From the first law of thermodynamics, the change in internal energy of the gas and of the liquid may be written, respectively, as

$$dE_g = C_{P_g}\, dT + \ell_{P_g}\, dP - P\, dV_g \qquad (19)$$

and

$$dE_\ell = C_{P_\ell}\,dT + \ell_{P_\ell}\,dP - P\,dV_\ell \tag{20}$$

Substitution of Equations 18, 19, and 20 into Equation 17 results in the following expression relating the change in enthalpy during vaporization of an infinitesimal weight of liquid to quantities which are measured experimentally.

$$\begin{aligned}\left(H_g - H_\ell\right)\left(\frac{-dm\,V_g}{V_g - V_\ell} - \frac{\left[m_g\,dV_g + m_\ell\,dV_\ell\right]}{V_g - V_\ell}\right)& \\ = q - m_g\left[C_{P_g}dT + \ell_{P_g}\,dP\right] - m_\ell\left[C_{P_\ell}\,dT + \ell_{P_\ell}\,dP\right] - \left[d\,\underline{E}_A\right]&\end{aligned} \tag{21}$$

Equation 21 must be integrated over the path of the vaporization process. Although it is expected that some temperature variation will occur, in practice it is possible to keep these variations small. Therefore, an average value of the enthalpy difference, $\left(H_g - H_\ell\right)_a$, may be assumed in the integration of Equation 21. Moreover, the initial and final temperatures in the vaporization process can be made identical within the precision of measurement. Under this condition, the integral of the final term on the right side of the equation becomes equal to zero. Furthermore it may be readily shown that the integral of the second expression in parenthesis on the left, under this condition, reduces to $(m_1 - m_2)\, V_g/(V_g - V_\ell)$. Therefore Equation 21, when integrated, becomes

$$(H_g - H_\ell)_a \, (m_1 - m_2) \frac{V_g}{V_g - V_\ell} = \underline{Q} - \int_{\theta_1}^{\theta_2} \left\{ (m_g C_{p_g} + m_\ell C_{p_\ell}) \left[\frac{dT}{d\theta}\right] d\theta + (m_g \ell_{p_g} + m_\ell \ell_{p_\ell}) \left[\frac{dP}{d\theta}\right] d\theta \right\} \tag{22}$$

Rearrangement of Equation 22 results in

$$(H_g - H_\ell)_a = \frac{V_g - V_\ell}{(m_1 - m_2)\, V_g} \left(\underline{Q} - \int_{\theta_1}^{\theta_2} \left\{ (m_g C_{p_g} + m_\ell C_{p_\ell}) \left[\frac{dT}{d\theta}\right] + (m_g \ell_{p_g} + m_\ell \ell_{p_\ell}) \left[\frac{dP}{d\theta}\right] \right\} d\theta \right) \tag{23}$$

In an actual vaporization process, either the gas or the liquid, or both, may be superheated. Designating the amount of superheat by ΔH , the change in enthalpy for the actual process may be written as

$$(H_g - H_\ell)_a = (H_d + \Delta H_g)_a - (H_b + \Delta H_\ell)_a \tag{24}$$

Equation 23 then becomes

$$\left(H_d - H_b\right)_a = \frac{V_g - V_\ell}{(m_1 - m_2) V_g} \left(\underline{Q} - \int_{\theta_1}^{\theta_2} \left\{ \left(m_g C_{P_g} + m_\ell C_{P_\ell}\right) \left[\frac{dT}{d\theta}\right] + \left(m_g \ell_{P_g} + m_\ell \ell_{P_\ell}\right) \left[\frac{dP}{d\theta}\right] \right\} d\theta \right) - \left(\Delta H_g\right)_a + \left(\Delta H_\ell\right)_a \tag{25}$$

If the temperature variation is sufficiently small, the integral in Equation 25 is negligible and averages are unnecessary so that Equation 25 becomes

$$H_d - H_b = \frac{\underline{Q}}{m_1 - m_2} \frac{V_g - V_\ell}{V_g} - \Delta H_g + \Delta H_\ell \tag{26}$$

For the case of an ideal process with no temperature variation or superheat involved, Equation 25 reduces to

$$H_d - H_b = \frac{\underline{Q}}{m_1 - m_2} \frac{V_d - V_b}{V_d} \tag{27}$$

DESCRIPTION OF APPARATUS

The calorimeter, used subsequently in this investigation, was built to measure heat capacities of liquids. During studies with corrosive materials, the instrument became badly corroded and unsuitable for use. In the present work, the calorimeter was repaired and modifications were made, extending its utility to vaporization studies as well as incorporating those changes desirable for heat capacity measurement.

Arrangement of Original Calorimeter Assembly

A detailed description of the apparatus, as originally assembled, has been presented (1). Much of the calorimeter and associated equipment was either unchanged or returned to its original status. The general arrangement of the original calorimeter assembly is shown in Figure 2. Since the parts shown represent little that is different, a detailed description of these parts will not be repeated here, although the legend accompanying the figure may be useful. The reader interested in the details is referred to Detailed Description of Apparatus in the Appendix.

In the original assembly, shown in Figure 2, the interior of the calorimeter A and the parts contained therein including the impeller B, the circulation shield D, and the guide vanes F, all of stainless steel, were gold plated. The gold plating had become loosened and was removed; those parts which had become corroded were repolished or replaced. The impeller B and the armature housing G had been mounted on platinum and glass bearings which were replaced with steel and bronze bearings. Pictures and diagrams which show the calorimeter and the associated equipment in more detail are included in the Appendix.

Circulation Shield

The circulation shield D, shown to scale in Figure 2, was modified by cutting ports in it to permit the circulation of samples having a total liquid volume appreciably less than the volume of the calorimeter (0.043 cubic foot). Capability of operation with smaller samples is important in vaporization studies since portions of the sample are withdrawn during operation. This feature is also important in heat capacity studies since one accurate method of evaluating this property involves measurement of the total heat capacity of the calorimeter and its contents using two different quantities of material in the system. The precision of the determination which is obtained by taking a difference, is influenced by the magnitude of the difference in quantity of material used in the two determinations.

The shield, without ports, is shown with other calorimeter parts in the photograph, Figure 6A, Appendix.

Calorimeter Heater

Complete submergence of the heater during vaporization studies is essential to avoid superheating of the gas phase. The original heater, which is not shown in Figure 2, was replaced by a more compact unit. The quantity of liquid sample required to cover the heater was thus reduced by approximately 30 per cent (0.0094 cubic foot).

The heater was constructed from approximately nine feet of No. 24 A.W.G. Chromel-A wire and was installed within a stainless-steel tube having an inside diameter of 0.055 inch. No. 24 A.W.G. copper wire leads, extending five inches within the calorimeter, were used for making the connections to the heater. Electrical energy to the heater was supplied by batteries and was controlled by means of a variable resistor in series with the heater. Potential leads, for measuring the voltage drop across the heater and the portion of the leads within the calorimeter, were connected at the exterior surface of the calorimeter. These potential leads, of No. 36 A.W.G. copper wire, were subsequently broken but were reconnected at points one inch from the external surface of the calorimeter.

The heater was insulated electrically from the steel tube by means of woven glass tubing. In order to insure good thermal conduction in the radial direction at both ends of the heater, packing comprised of Alundum cement and plaster of Paris was inserted in the space between the electrical leads or the heater wire and the outer steel tube along a length of one foot from the inner wall of the calorimeter.

The ends of the steel tube, which passed through the wall of the calorimeter by means of sealed connections, were open to the vacuum chamber. The leads to the heater entered the vacuum chamber through a vacuum line. A differential two-junction thermocouple was installed on one of the heater leads in order to determine the temperature gradient between two points along the lead. All wires entering the vacuum chamber, including the heater leads, were insulated with a double layer of fiber-glass and were cemented to the wall of the vacuum jacket J, Figure 2, to reduce the differences between the temperatures of the wires and the temperature of the jacket.

Thermometer Well

The tube containing the resistance thermometer E, shown in Figure 2, was replaced with the closed thermometer well shown in Figure 3. This arrangement provided for the withdrawal of the gas phase from the top of the calorimeter, and permitted the operation of the resistance thermometer in a gas atmosphere. A photograph, Figure 4, shows an exploded view of the thermometer well and accessory parts.

Tube for Thermometer Leads

The leads from the resistance thermometer E, Figure 2, were enclosed within a thin-walled stainless-steel tube having an outside diameter of 0.093 inch. The tube, entering the vacuum line from the vacuum chamber, was soldered to a copper junction block to give good thermal contact with the vacuum line at the place where the vacuum line was connected to the vacuum jacket.

The path followed by the tube from the top of the calorimeter to the junction block was approximately 18 inches in length and is shown in the photograph, Figure 5. In addition to this measure for guarding against heat losses, a heating element was wound around the tube within the chamber, about one inch from the junction block. The heater, which was wound non-inductively, was manually controlled by means of a variable autotransformer in series with an isolation transformer used as the power supply. A differential two-junction thermocouple with one junction near the heater and the other near the calorimeter aided in adjusting the temperature gradient to approximately zero.

The tube with the thermometer leads passed from the vacuum system through a fitting and terminated in a small chamber. The wires passed from the chamber through a wax seal which closed the top of the chamber. The chamber, equipped with a pressure gauge, served as a reservoir for helium which surrounded the thermometer. The chamber and some of the instrument wiring are shown in the photograph, Figure 6.

Tube for Vapor Withdrawal

The vapor phase was withdrawn from the top of the calorimeter through a tube by the arrangement shown in Figure 3. The withdrawal tube, of stainless steel and having an outside diameter of 0.072 inch, passed from the calorimeter, through the vacuum chamber and the vacuum line in a manner similar to that described for the tube carrying the thermometer leads. A guard heater and differential thermocouple were also installed along this tube in the same manner as on the tube carrying the thermometer leads. The vapor-carrying tube left the vacuum line through a suitable fitting and terminated in a valve block located close to the fitting. The section of tube within the vacuum system was suspended from the fitting, the junction block, and the calorimeter, making no other contact with the surroundings.

The sections of tube between the valve block and the vacuum fitting, and between the vacuum fitting and the vicinity of the junction block, were each clad with a close-fitting section of copper tubing having an outside diameter of 1/8 inch. Heaters for use in controlling the temperature of the vapor tube were wound on the copper tube and on the vacuum fitting in order to prevent condensation of the vapor within the tube. The portion of copper tubing within the vacuum line was wound along two sections with separate heaters. The wiring in these heaters was distributed in such a manner that the heat flux at any point closely matched the calculated loss by radiation at the highest operating temperature of the equipment. The heater on the section of tubing between the vacuum fitting and the valve block was wound uniformly. This section of tubing and the vacuum fitting were also thermally insulated with fiber-glass. Each heater was non-inductively wound and was controlled manually with an autotransformer in series with an isolation transformer.

The temperature of the two heated sections within the vacuum line could be compared with the temperature of the vacuum jacket at a point well removed from the vacuum line by means of differential two-junction thermocouples. The temperature of the vacuum fitting and of the section of the vapor line between the fitting and the valve block could be compared in the same manner with the temperature at a point within the tube enclosing the leads to the resistance thermometer about one inch from the calorimeter.

Orifice Block

The rate of removal of vapor was controlled by three orifices, located within the orifice block, which could be used separately or in combination. Five orifice sizes were used, ranging from 0.0044 to 0.020 inch in diameter. The area ratios of two successive orifice sizes in the series were approximately one half. The details of the orifice block are shown in Figure 7. A view of the two largest orifice plates is shown in Figure 8.

The temperature of the orifice block was controlled by means of a heater. The heater on the orifice block was non-inductively wound and was controlled manually in the same way as were the heaters on the tubes described above. A differential two-junction thermocouple was employed in controlling the temperature of the orifice block and utilized the same reference junction used for setting the temperature of the vacuum fitting and adjacent section of tubing.

The orifice block was mounted with steel studs on a transite wall. Thermal insulation from the surroundings was provided by surrounding the orifice block with glass wool, shielded against convection currents by a bakelite box with thin walls. Views of the orifice block showing the installation are seen in the photographs, Figures 9 and 10.

Withdrawal Manifold

Two weighing bombs, used as condensers, could be readily coupled to the vapor-withdrawal manifold which was joined to the orifice block with a section of copper tubing of 3/16 inch outside diameter. No heaters were installed on the withdrawal manifold or on the section of copper tubing connecting the manifold and the orifice block. The withdrawal manifold, with two weighing bombs attached is shown in the photograph, Figure 11.

Calorimeter Thermocouple Location

Three differential two-junction thermocouples, each with one junction mounted on the interior surface of the jacket, were installed to compare the temperature of the calorimeter A at three different locations, with the temperature of the jacket J, Figure 2. The junctions located on the exterior surface of the calorimeter were installed at points corresponding to the elevation of the surface of the liquid in the calorimeter when the calorimeter is approximately one-third, one-half and two-thirds full, respectively. A differential two-junction thermocouple was installed within the thermometer well, Figure 3, with one junction located near the top and the other approximately 3.1 inches lower.

Temperature Measurement

The temperature of the oil bath, K, Figure 2, in relation to the International Platinum Scale, was determined by means of a strain-free platinum resistance thermometer of the coiled filament type (12). The thermometer was calibrated by comparison with an equivalent instrument calibrated by the National Bureau of Standards. A similar device was used to measure the temperature of the calorimeter and its contents.

The resistances of the two platinum resistance thermometers were measured with Mueller bridges using conventional four-lead connections. The temperature, measured by this method, was known to within 0.02°F in relation to the International Platinum Scale. Changes in temperature could be measured with an uncertainty of not more than 0.003°F.

Voltage Measurement

A White double potentiometer was used to measure the voltages of those thermocouples having both junctions mounted within the vacuum jacket. The uncertainty in the voltage measurements was about 0.1 microvolt. Thermocouples having both junctions within the vacuum jacket include those used to measure the temperature difference between the calorimeter and the jacket, those used to measure temperature gradients along the tubes leaving the top of the calorimeter and along one heater lead, and the thermocouple within the thermometer well.

The thermocouples having only one junction within the vacuum jacket were used to control the temperature along the path followed by the vapor leaving the calorimeter. A Leeds and Northrup Student Potentiometer was used to measure the voltages of these thermocouples. The uncertainty in the voltage measurements, in this case, was approximately 2 microvolts.

Voltage measurements, for evaluating the power input to the heater in the calorimeter, were made with a Type K-2 potentiometer (Leeds and Northrup) with an estimated uncertainty of not more than 0.02 per cent.

Time Measurement

The time readings, required in evaluating the energy added to the heater by integration of the power input, were taken from a synchronous electrical timer, using the frequency of the alternating current in the laboratory as a standard. Time intervals were measurable to within ± 0.01 of a second. The timer was located near the instruments used for measuring and adjusting the current in the calorimeter heater; the timer switch was strategically situated near the weighing bombs. The operations of adjusting the current in the heater circuit and of diverting the flow of vapor into a new receiver while simultaneously actuating the timer switch could be carried out quickly. It is estimated that the uncertainty in any time determination was approximately 0.2 second.

Temperature Control

The temperature of the oil bath K, Figure 2, was controlled automatically by means of a modulating electronic circuit (13) operating in conjunction with the resistance thermometer in the bath. All other temperatures were controlled manually. The control of the temperature along the path followed by the withdrawn vapor was facilitated by drawing the requisite power for the appropriate heaters from a voltage stabilizer.

Agitator-Drive Motor

The energy added mechanically to the calorimeter should be small compared to the energy added electrically.

The motor originally installed to drive the agitator was replaced with a synchronous inductor motor in order to reduce the speed of the agitator from approximately 160 revolutions per minute to approximately 32 revolutions per minute. The motor used for replacement was undersized and was used pending the installation of a suitable motor.

ENERGY CALCULATIONS

Energy was added electrically to the calorimeter by means of a heater and mechanically by means of an agitator. In addition, some energy transfer was involved between the calorimeter and the surrounding jacket (viz., by conduction and radiation) as a result of temperature differences between the surface of the calorimeter and the surface of the surrounding jacket.

Energy Added Electrically

The energy added by the heater was determined from measurements of the voltage drop across the heater and the current, taken at regular time intervals during the vaporization process. The voltage drop across the heater was established from measurements of the potential drop across a section of a large calibrated resistor placed in parallel with the heater. The large resistor, of approximately 10^4 ohms, was made of manganin wire on account of the low temperature coefficient of electrical resistance of this material, and was calibrated against a standard resistor obtained from the Leeds and Northrup Company. The current through the circuit was determined by measuring the potential drop across a standard resistor in series with the heater. The extent of uncertainty in the values of the resistances was less than 0.02 per cent. The uncertainty involved in evaluating the power input to the heater was less than 0.04 per cent. The time readings could be obtained with a maximum error of 0.2 second. From the above, it is estimated that the amount of energy added by the heater, obtained by the integration of the power input over the duration of the vaporization process, was known with an uncertainty of not more than 0.06 per cent. The details of the heater circuit and of the calculation of energy added electrically to the calorimeter are presented in the Appendix.

Energy Added Mechanically

The rate of energy addition to the calorimeter by the agitator was evaluated by measuring the rate of rise of temperature of the calorimeter as a result of the operation of the agitator. This rate was compared with the rate of rise under the same conditions but with a known rate of addition of electrical energy. The comparison was made for conditions of zero temperature difference between the calorimiter and the surrounding jacket. Representative curves for this calibration are shown in Figure 12.

The rate of addition of energy by the agitator varies with the speed of rotation of the agitator and with the viscosity, specific weight, and quantity of the fluid in the calorimeter. Therefore, the agitator was operated at a constant speed and the rate of energy addition was evaluated throughout the temperature range of the investigations. The amount of variation in the quantity of fluid in the calorimeter was small; the effect on the value of the rate of energy addition was found to be less than the uncertainty involved in the evaluation of the energy addition rate and therefore was neglected. It is believed that the uncertainties in the values for the rate of energy added mechanically were not greater than 10 per cent. Since the energy added mechanically during the vaporization process was as much as 2 per cent of that added electrically, the uncertainty in the total energy added, introduced by the agitator, amounted to as much as 0.2 per cent. The calibration data for the rate of addition of energy by the agitator, and a sample calculation of the amount of energy added by this means are included in Discussion of Agitator Energy, Appendix.

Energy Transfer between Calorimeter and Jacket

The gain or loss of energy by the calorimeter as a result of thermal transfer by conduction and radiation between the calorimeter and the surrounding jacket was assumed, for any given temperature, to be directly proportional to the average temperature difference.* The energy exchange between the calorimeter and the jacket during the period of interest may be expressed by the relationship:

$$Q_J = \int_{\theta_1}^{\theta_2} k \left(T_J - T_A\right) d\theta \qquad (28)$$

The constant of proportionality, k, of Equation 28 was determined by applying Equation 28 to an actual case in which a known quantity of energy was exchanged by thermal transfer under conditions approximating those of the vaporization studies. The average of the temperatures

---

*This assumption is not in general agreement with Stefan's law which states that the transfer of energy by radiation is proportional to the difference of the absolute temperatures raised to the fourth power. However, when the temperature difference is small, the difference of the temperatures to the fourth power may be approximated in terms of an average temperature, T_a, and the temperature difference as follows:

$$T_J^4 - T_A^4 = \left(T_J^2 + T_A^2\right)\left(T_J + T_A\right)\left(T_J - T_A\right)$$

and

$$T_J^4 - T_A^4 \simeq 4 T_a^3 \left(T_J - T_A\right)$$

indicated by the resistance thermometers in the oil bath surrounding the jacket and in the calorimeter was taken as the average temperature, T_a . In using Equation 28 it was convenient to express the temperature difference and the proportionality constant in terms of resistance units rather than temperature units.

A typical cooling curve, interrupted by the addition of a known quantity of energy, is shown in Figure 13 for a calibration carried out at 310°F. Equation 28 was applied over the time interval from θ_3 to θ_4 . A calibration was also carried out at 130°F. Values of the proportionality constant at other temperatures of interest were obtained by linear interpolation or extrapolation of the values obtained experimentally.

It is believed that the values of the proportionality constant obtained experimentally are known to within 4 per cent and that other values are uncertain by not more than 10 per cent. The energy transferred to or from the calorimeter by thermal exchange with the jacket, during vaporization studies, did not exceed 0.06 per cent of the energy added electrically, and thus introduced an uncertainty of not more than 0.006 per cent in the total energy added. The Appendix includes the calibration data and a sample calculation for the energy exchange between the calorimeter and the vacuum jacket.

MATERIALS

The n-heptane and the n-octane used in these studies were obtained from the Phillips Petroleum Company. The n-heptane was pure grade, containing 99 mole per cent n-heptane. The supply of n-octane was research grade and contained 99.83 mole per cent of n-octane. The materials were dried over metallic sodium and used without further purification except for deaeration. Dissolved air was removed by freezing the materials, using liquid nitrogen as the refrigerant, and subsequent evacuation. This operation was repeated until the pressure above the frozen material was constant for two successive operations.

The index of refraction of the n-octane sample at 68°F, relative to the sodium D lines, was 1.3973 as compared with 1.39743 reported by Rossini (14). At 68°F, the specific weight of the n-octane was 43.8617 pounds per cubic foot as compared with a value of 43.856 pounds per cubic foot by Rossini (15). The impurities in the n-octane were reported to be largely isoparaffins and other compounds having latent heats of vaporization not greatly different from that of the sample. It is believed that the uncertainty introduced into the determination of the latent heat of vaporization of n-octane, as a result of the impurities, is negligible.

PROCEDURE

Transfer of Material into Calorimeter

The operation of transferring the material being investigated into the apparatus was performed by first evacuating the apparatus. The material was then distilled into the apparatus in such quantity that, during the investigation, the surface of the liquid was well above the heater and the gas phase occupied at least 20 per cent of the volume of the calorimeter. A record was maintained of the amount of material which was contained within the apparatus, and subsequent additions were made when necessary.

Preliminary Operations

The actual vaporization process was preceded by a number of operations designed to attain the desired conditions within and in close proximity to the apparatus. The jacket and the calorimeter were brought to the selected temperature and the guard heaters were adjusted to give nearly zero temperature gradients along the tubes leading from the top of the calorimeter. The temperature along the path followed by the vapor in passing from the vacuum jacket to the orifices was adjusted to approximately 5°F above the temperature in the calorimeter. Two weighing bombs, serving as condensers for the withdrawn gas, were attached to the vapor-receiving manifold. The appropriate lines were evacuated and the weighing bombs were cooled by contact with liquid nitrogen. The agitator and heater within the calorimeter were started, and a valve to one of the weighing bombs and one or more of the orifice valves were opened. The rate of energy addition to the heater was adjusted until the temperature of the calorimeter remained nearly constant and was close to that of the jacket. A withdrawal rate, in the approximate range between 0.2 and 0.6 gram of sample per minute, was selected such that the heater current was between 0.25 and 0.50 ampere.

Vaporization Run

When the vaporization was proceeding smoothly at the desired temperature, the flow of vapor was diverted to the second weighing bomb and the timer was started. The timer switch was strategically situated near the weighing bomb; this facilitated the crucial operation of simultaneously diverting the flow into a new receiver and starting the timer. During the vaporization run, readings of the current to and the voltage across the calorimeter heater were taken alternately at intervals of from one to two minutes. Frequent readings were taken of the temperature of the calorimeter, the temperature of the jacket, and the temperature difference existing between the calorimeter and the jacket. Readings were also taken of the temperatures of the outgoing gas and along the withdrawal line, and of the temperature gradients along the tubes and one heater lead between the calorimeter and the jacket. Manual adjustments of the appropriate heaters were made, as required, to maintain the temperatures within acceptable limits. The times of the readings as well as of heater adjustments were noted and recorded. The adjustment of current through the heater in the calorimeter was made at times of even seconds noted on the timer. After a minimum of 10 grams of the material had been withdrawn, the flow of gas was diverted back to the original weighing bomb and the timer was stopped. The valves to the orifices were closed and the heaters and agitator were turned off. The weight of sample collected during the run was determined from the initial and final weights of the second weighing bomb.

Control of Operating Conditions

The temperature of the oil bath and vacuum jacket was maintained constant, to within approximately 0.01°F, during the vaporization processes. The maximum variation in temperature of the calorimeter during any investigation was 0.05°F and the average of the maxima for all of the determinations was less than 0.02°F. The temperature of the calorimeter at the end of a vaporization process, owing to corrective measures taken near the end of the run, was always identical, within the precision of temperature measurement (0.003°F), with the temperature at the start of the run.

The identity of the initial and final temperatures made it unnecessary to know the heat capacity of the calorimeter and the weight of the material in the liquid and the gas phases. A typical curve illustrating the variation of temperature with elapsed time during an actual process is shown in Figure 8. The power input to the calorimeter heater is also shown over the same time interval.

The difference in temperature between the liquid in the calorimeter and the exit gas varied between approximately 0.1 and 0.4°F depending upon the rate of vaporization, but was substantially constant during any single investigation.

EVALUATION OF LATENT HEAT OF VAPORIZATION FROM EXPERIMENTAL DATA

Values of the latent heat of vaporization were calculated from the experimental data by means of Equation 26. The effect of the temperature variations during any investigation was calculated to be less than the effect of the uncertainty involved in measurement of temperature and was neglected. The uncertainty introduced by neglecting the effect of temperature variations amounted to less than 0.003 per cent. Equation 25, rather than Equation 26, is used when this effect is considered.

Energy Evaluation

The amount of electrical energy added to the calorimeter was obtained by integration of the area under the power curve, Figure 14. The energy added mechanically by the agitator was evaluated by taking the product of the time interval of vaporization and the power of the agitator, obtained by calibration. Energy gained or lost by thermal transfer between the calorimeter and the vacuum jacket was obtained by graphical integration utilizing Equation 28. Energy lost from the calorimeter by thermal transfer along the heater leads was established separately from the measured temperature gradient.

Weight of Material Withdrawn

The material withdrawn from the calorimeter during a vaporization run was condensed in a weighing bomb. The weight of material withdrawn was determined directly by weighing the bomb before and after the withdrawal.

Volumetric Correction

The specific volume of liquid n-heptane, required for the volumetric correction in Equation 26, was taken from the literature (16); the specific volume of the saturated gas was obtained from unpublished data available in this laboratory (17). In the case of n-octane, the specific volume of the liquid was taken from the data of Young (8). The specific volume of the saturated gas was obtained by the simultaneous solution of Equation 26 and the Clapeyron equation, using the vapor pressure data of Young. The values of the volumes resulting were extrapolated to the lower temperatures of interest by means of a plot of compressibility factor vs. temperature; the results are listed in Table I. The volumetric correction in Equation 26 amounted to less than 2 per cent of the latent heat of vaporization.

Superheat Correction

In evaluating equation 26, it was assumed that the vaporization took place at the temperature of the gas phase and that the liquid was superheated. The temperature difference between the gas and liquid was taken to be that indicated by the thermocouple within the thermometer well. The correction for superheat may be shown to be equal to the product of the isobaric heat capacity of the liquid and the average amount of superheat. The isobaric heat capacity of n-heptane at bubble-point was obtained from the literature (18). The isobaric heat capacity of n-octane at bubble-point was estimated by means of the following equation:

$$C_{p_g} - C_{p_\ell} = \frac{d\left(H_d - H_b\right)}{dT} + V_\ell \frac{dP''}{dT} \qquad (29)$$

Equation 29 may be derived by assuming that the vapor behaves as a perfect gas and that the rate of change of volume of the liquid with temperature is zero. The maximum correction for superheat amounted to less than 0.15 per cent of the value of the latent heat of vaporization.

RESULTS

The latent heat of vaporization of n-heptane was determined only at 100°F. The result, 153.6 Btu/lb, was about 0.09 per cent larger than the corresponding value obtained by interpolation of the values found in the literature (3,4,5,6,7,8) as shown in Figure 15.

The latent heat of vaporization of n-octane was determined at nine temperatures in the range from 100 to 340°F. The experimental points, with a smooth curve drawn through them, are shown in Figure 16. The experimental points, together with the corresponding values read from the curve, are recorded in Table II. The deviations of the experimental values from the smooth curve are also included in the table. The average deviation without regard to sign was calculated to be 0.17 per cent and the standard deviation was found to be 0.27 per cent.

A comparison of the results of this investigation with the values of the latent heat of vaporization of n-octane reported in the literature (3,6,8,9) is shown in Figure 16. The results of this investigation are in excellent agreement with the measurements of Osborne and Ginnings (3) at 77°F. Agreement with the reported values of others at higher temperatures is fair.

The difference in internal energy of saturated gas and saturated liquid was calculated for n-octane in the temperature range from 100 to 340°F from the values of the latent heat of vaporization from Table II, the specific volume of the saturated gas, Table I, values of the specific volume of the saturated liquid from Young (8), and the vapor pressure from Rossini (6) and Young (8). The results of these calculations are recorded in Table III.

In Table IV, values of the more important variables of interest in a vaporization process are listed for each of the vaporization runs with n-octane. Values given in the table are temperature, duration of process, electrical energy added, energy added by agitator, energy gained by thermal transfer from surroundings, net energy added, weight of material withdrawn, and average superheat of liquid. Also included in the table are average power input, size of orifice used, and average withdrawal rate.

The errors involved in the present work are primarily those associated with evaluation of the energy added to the calorimeter. It is believed that the high vacuum and weighing bomb technique (19) for establishing the weight of material withdrawn is accurate and that the probable error in the final result introduced by the weighing of material withdrawn is less than 0.02 per cent. The limitations in precision of temperature measurement introduce an uncertainty of as much as 0.08 per cent due to uncertainty in the total energy of the calorimeter and its contents. The errors involved in evaluating the correction terms of Equation 26 are not significant. The significant contributing errors are listed below.

Quantity	Possible error, %
Electrical energy	0.05
Agitator energy	0.2
Energy exchange between calorimeter and jacket	0.006
Change in temperature	0.08
Weight of material withdrawn	0.02

The predicted standard deviation, based on these estimates of the errors involved as standard deviations, is 0.22 per cent. The actual standard deviation of the experimental results is slightly greater than predicted. It is supposed, however, that an additional possible source of error attributable to condensation of the material in the vapor withdrawal tube or in the valve block, could account for a greater deviation. All of the experiments below 310°F were made prior to the installation of the voltage stabilizer in the power supply circuit to the heaters used to prevent such condensation.

Barring any errors due to condensation, the agitator is the greatest source of error. The calibration procedure used to evaluate the energy input by the agitator is simple in principle. However, in practice, high accuracy is difficult to achieve since a small temperature increment is measured and consequently limitations in the precision of temperature measurement result in an appreciable relative error. In addition, in this work, the motor for the agitator drive was undersized and part of the difficulty in the agitator calibration resulted from random slipping of the motor. A motor of suitable size was subsequently obtained for use as a replacement.

It is concluded that the apparatus functions according to design and that the results obtained are in very good agreement with the best data from the literature.

RECOMMENDATIONS

It is recommended that one of the differential thermocouples within the jacket be moved to provide a more reliable measure of the difference in temperature between the liquid and gas phases. The junction referring to the gas phase should be placed on the withdrawal tube at a point close to the calorimeter. The thermocouple used to measure the temperature gradient along one of the heater leads could serve this purpose since the temperature gradient along the lead could be related, by calibration, to the power input to the heater.

Electrically operated, quick opening valves could be used advantageously for diverting the flow of the withdrawn vapor. The simplest arrangement would utilize a single 3-way valve. Such valves, operated by solenoid, are commercially available. The result of such an installation should be the improved measurement of the duration of a vaporization run.

The use of an injector for the addition of material to the calorimeter would save a considerable amount of time during a series of vaporization studies. The present procedure of introducing the material by distillation requires that the calorimeter not be hot during the operation. Since cooling and reheating to operating conditions is time consuming, much loss of time could be avoided.

REFERENCES

1. Sage, B. H. and Hough, E. W., "A Calorimeter for Corrosive Liquids," Jet Propulsion Laboratory Progress Report No. 1-52, California Institute of Technology, Pasadena, California, 1947.
2. *Chem. Eng. News*, 27, 2727 (1949).
3. Osborne, N. S. and Ginnings, D. C., *Bur. Std. J. Research*, *39*, 453 (1947).
4. Pitzer, K. S., *J. Am. Chem. Soc.*, *62*, 1224 (1940).
5. Mathews, J. H., *J. Am. Chem. Soc.*, *48*, 562 (1926).
6. Rossini, F. D., *et al.*, "Selected Values of Physical and Thermodynamic Properties of Hydrocarbons," p. 435, Carnegie Press, Pittsburgh, Pa., 1953.
7. Waddington, G., Todd, S. S. and Huffman, H. M., *J. Am. Chem. Soc.*, *69*, 22 (1947).
8. Young, S., Sci. *Proc. Royal Dublin Soc.*, *12*, 374 (1910).
9. Barrow, G. M., *J. Am. Chem. Soc.*, *73*, 1825 (1951).
10. Osborne, N. S., Stimson, H. F. and Fiock, E. F., *Bur. Std. J. Research*, *5*, 411 (1930).
11. Osborne, N. S., Stimson, H. F. and Ginnings, D. C., *Bur. Std. J. Research*, *23*, 197 (1939).
12. Meyers, C. H., *Bur. Std. J. Research*, *9*, 807 (1932).
13. Sage, B. H. and Lacey, W. N., *Trans. Am. Inst. Mining and Met. Engrs.*, *136*, 136 (1940).

14. Rossini, F. D., loc. cit., p. 34.

15. Rossini, F. D., ibid., p. 98.

16. Nichols, W. B., Reamer, H. H., and Sage, B. H., Ind. Eng. Chem., 47, 2219 (1955).

17. Derived Data Book #1277, p. 31, Department of Chemical Engineering, California Institute of Technology, Pasadena, Calif.

18. Douglas, T. B., Furukawa, G. T., McCoskey, R. E., and Ball, A. F., Bur. Std. J. Research, 53, 139 (1954).

19. Sage, B. H. and Lacey, W. N., loc. cit.

20. Hodgman, C. D., "Handbook of Chemistry and Physics," Chemical Rubber Publishing Co., 35th Edition, p. 2361.

NOMENCLATURE

C_p	specific heat capacity at constant pressure
d	differential operator
E	specific internal energy
$\underline{E}$	total internal energy
k	constant of proportionality
ℓ_p	latent heat of pressure change
m	weight of material within calorimeter
P	pressure
P''	pressure in two-phase region
q	infinitesimal amount of energy
$\underline{Q}$	energy added to calorimeter
t	temperature
T	thermodynamic temperature
V	specific volume
$\underline{V}$	total volume
$\underline{w}$	infinitesimal amount of work
θ	time
ΔH	finite increment of superheat

Subscripts

A	calorimeter
a	average
b	bubble-point liquid
d	dew-point gas

NOMENCLATURE (cont.)

Subscripts

e	electrical
g	gas
J	vacuum jacket
ℓ	liquid
s	agitator
1	initial
2	final
3	initial, calibration of k
4	final, calibration of k

Superscript

$'$	pertains to material transferred across boundary of system

LIST OF FIGURES

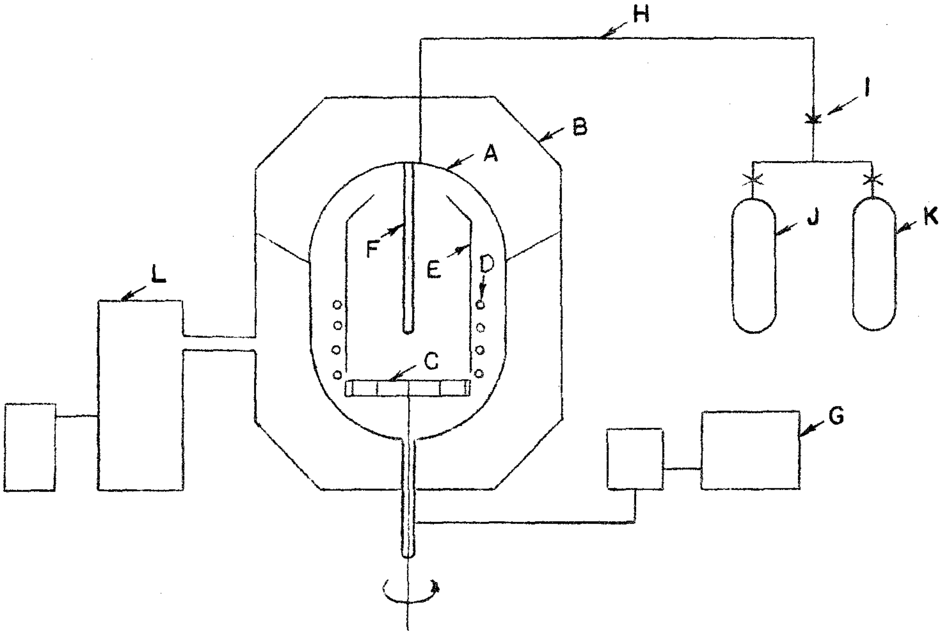

Figure 1. Schematic Arrangement of Equipment

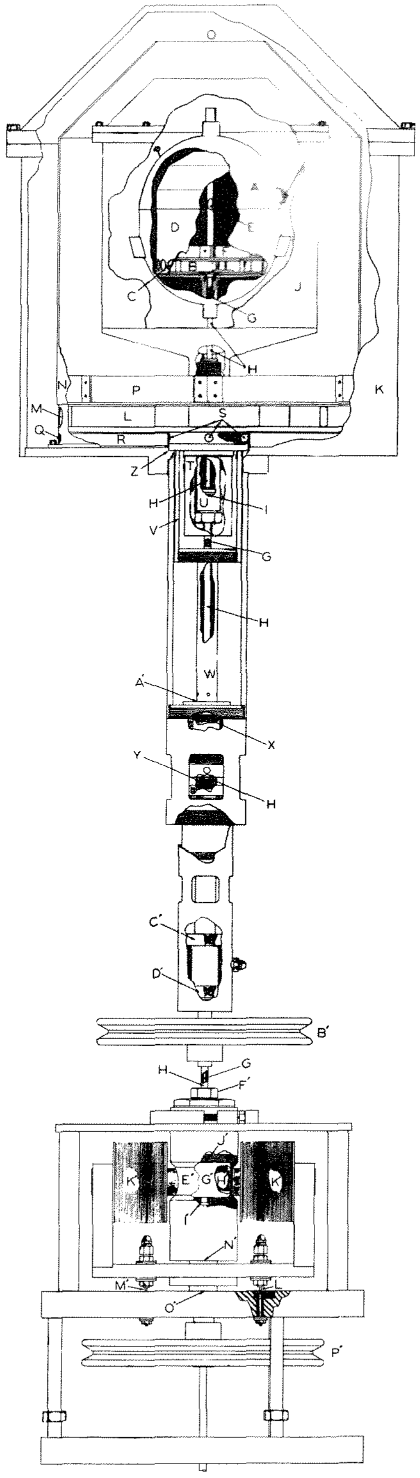

Figure 2. General Arrangement of Equipment

LEGEND - Figure 2

A	calorimeter
B	agitator
C	ports in circulation shield D
D	circulation shield
E	resistance thermometer
F	radial guide vanes
G	drive shaft for the agitator B
H	tube
I	seal between tube H and sleeve U
J	vacuum jacket
K	oil bath
L	impeller
M	ports in circulation shield N
N	circulation shield
O	opening in circulation shield
P	radial guide vanes
Q	ports in path Q-R-S-T
R	guide vanes
S	ports
T	circulation shield
U	sleeve--part of vacuum jacket
V,W	sleeve--part of drive for the impeller L
X	packing gland through which the sleeve W leaves the oil bath

LEGEND - Figure 2 (cont.)

Y	packing gland through which the tube H leaves the oil bath
A'	bearing
B'	pulley
C',D'	support bearings for the pulley B'
E'	steel shell
F'	sealing nut between tube H and shell E'
G'	armature housing
I',J'	steel--bronze bearings in which the armature housing rotates
K'	electromagnets
L',M'	slip rings through which the electromagnets are energized
N',O'	support bearings for the electromagnet assembly
P'	pulley to drive the electromagnet assembly

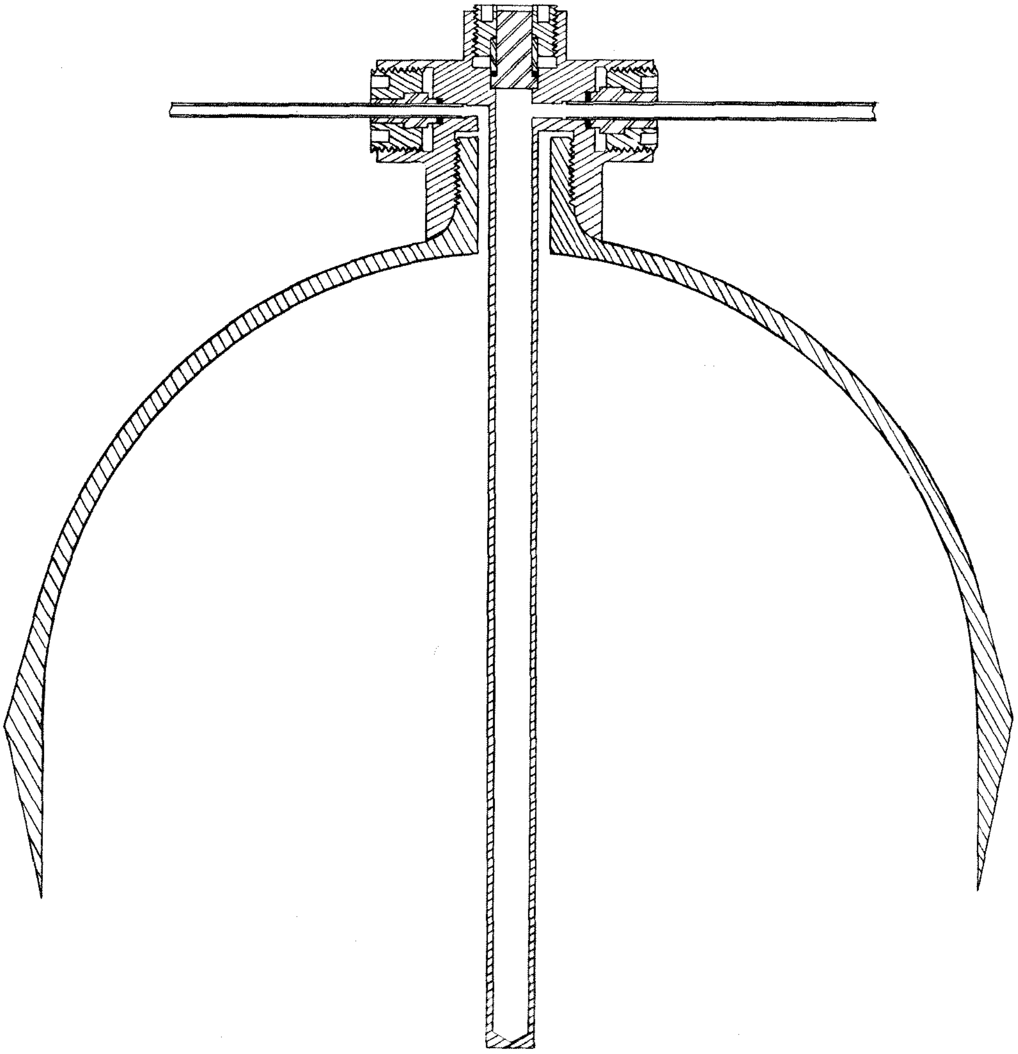

Figure 3. Thermometer Well

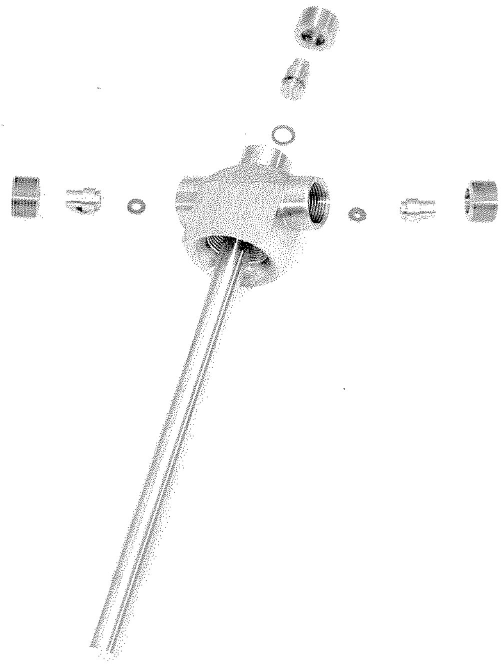

Figure 4. Thermometer Well and Accessory Parts--
Exploded View

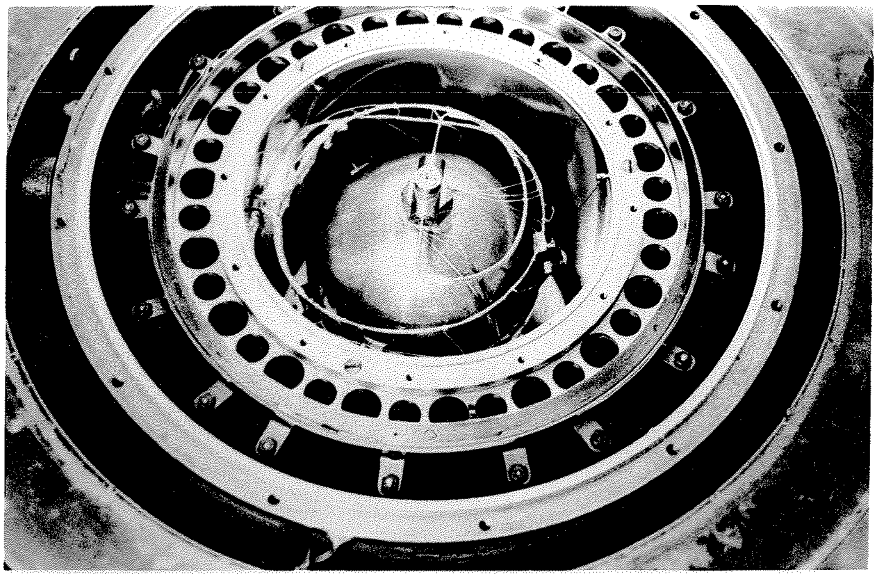

Figure 5. View Showing Paths of Tubes from Top of Calorimeter

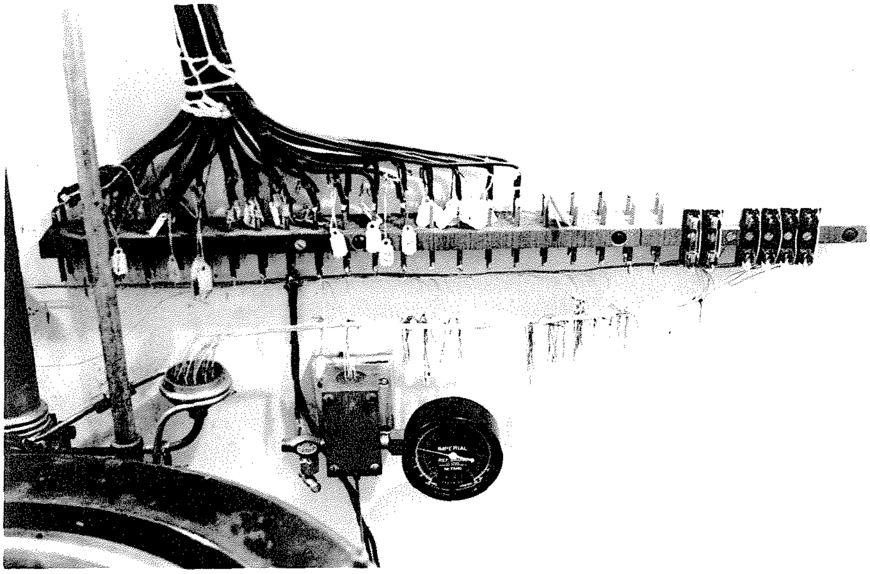

Figure 6. **Instrument Wiring and Helium Reservoir**

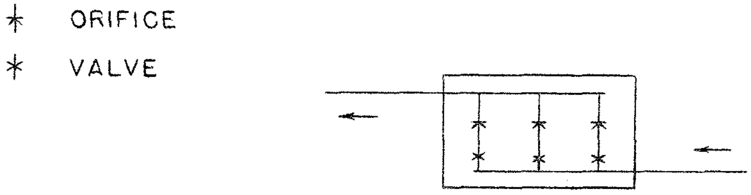

FLOW WITHIN ORIFICE BLOCK
(FRONT VIEW)

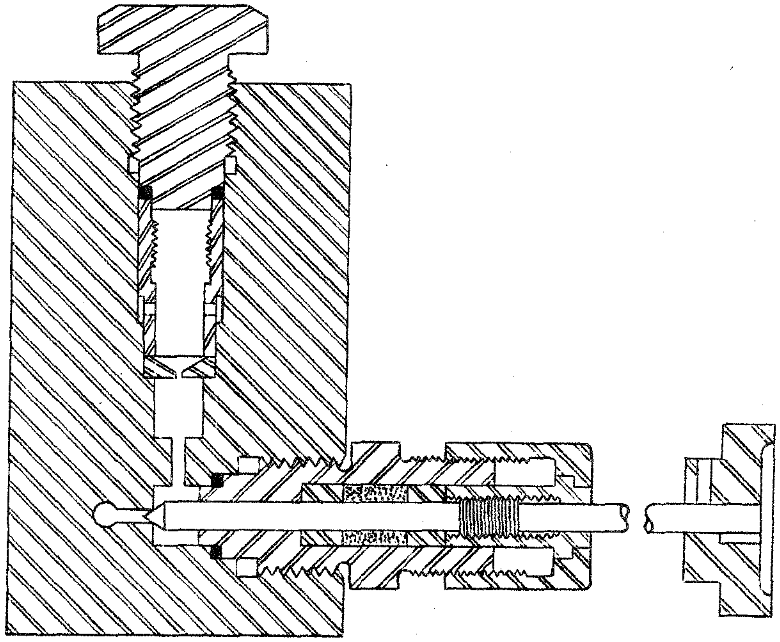

SIDE SECTION

Figure 7. Details of Orifice Block

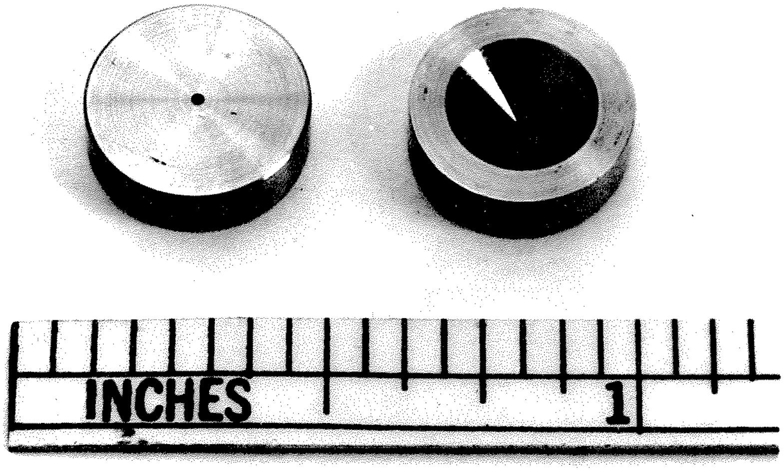

Figure 8. Orifice Plates

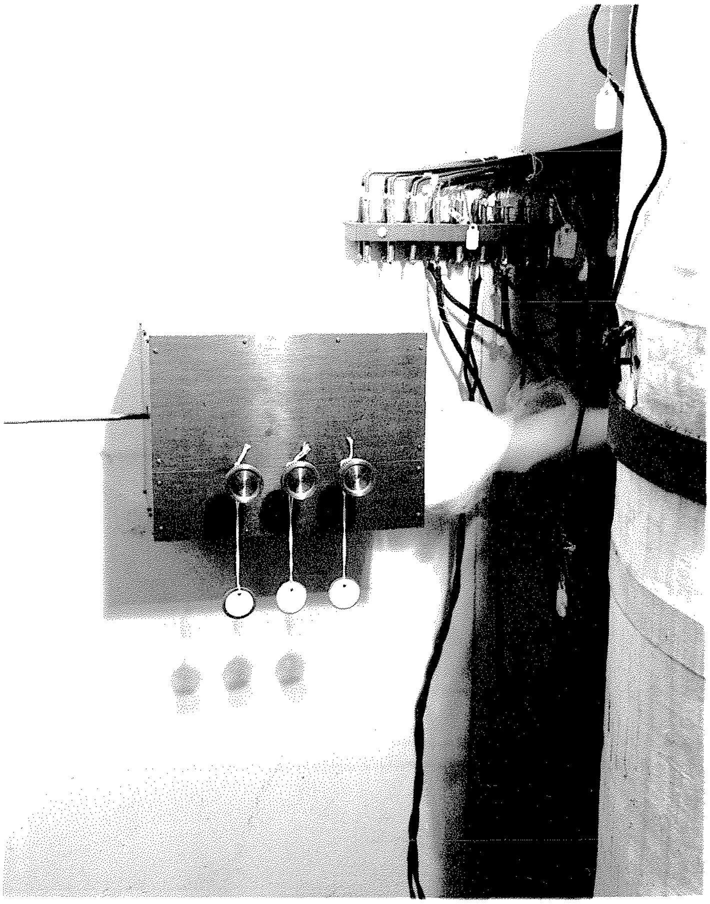

Figure 9. **Orifice Block Installation**

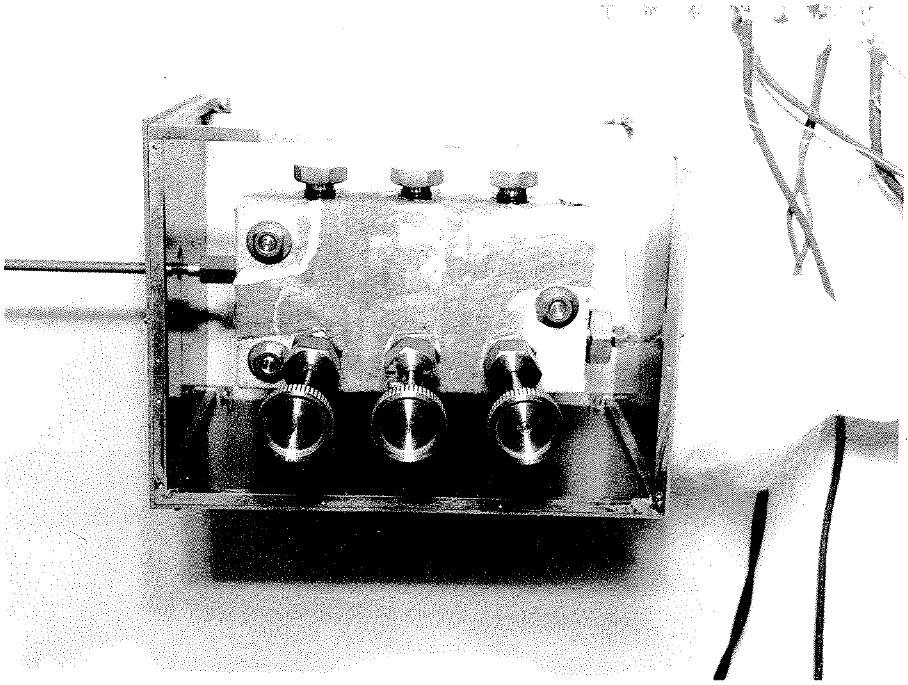

Figure 10. Orifice Block

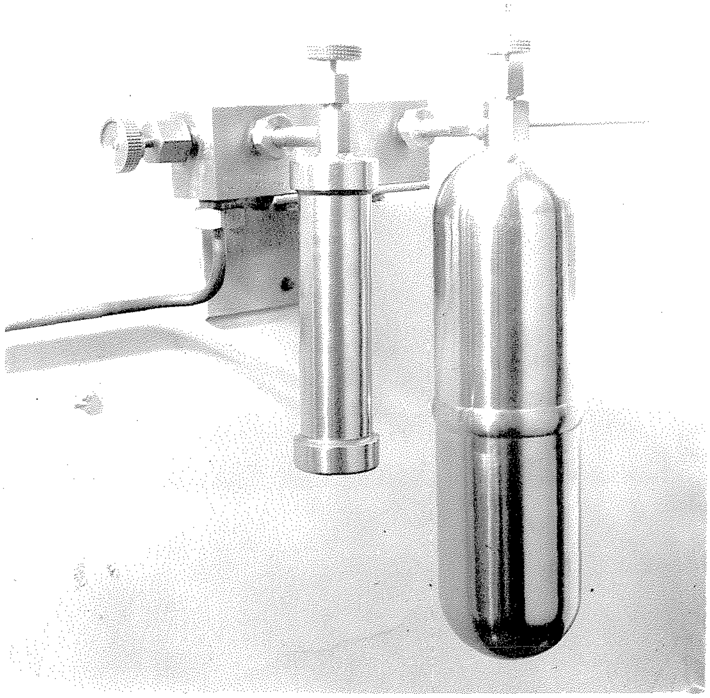

Figure 11. Withdrawal Manifold and Weighing-Bomb Condensers

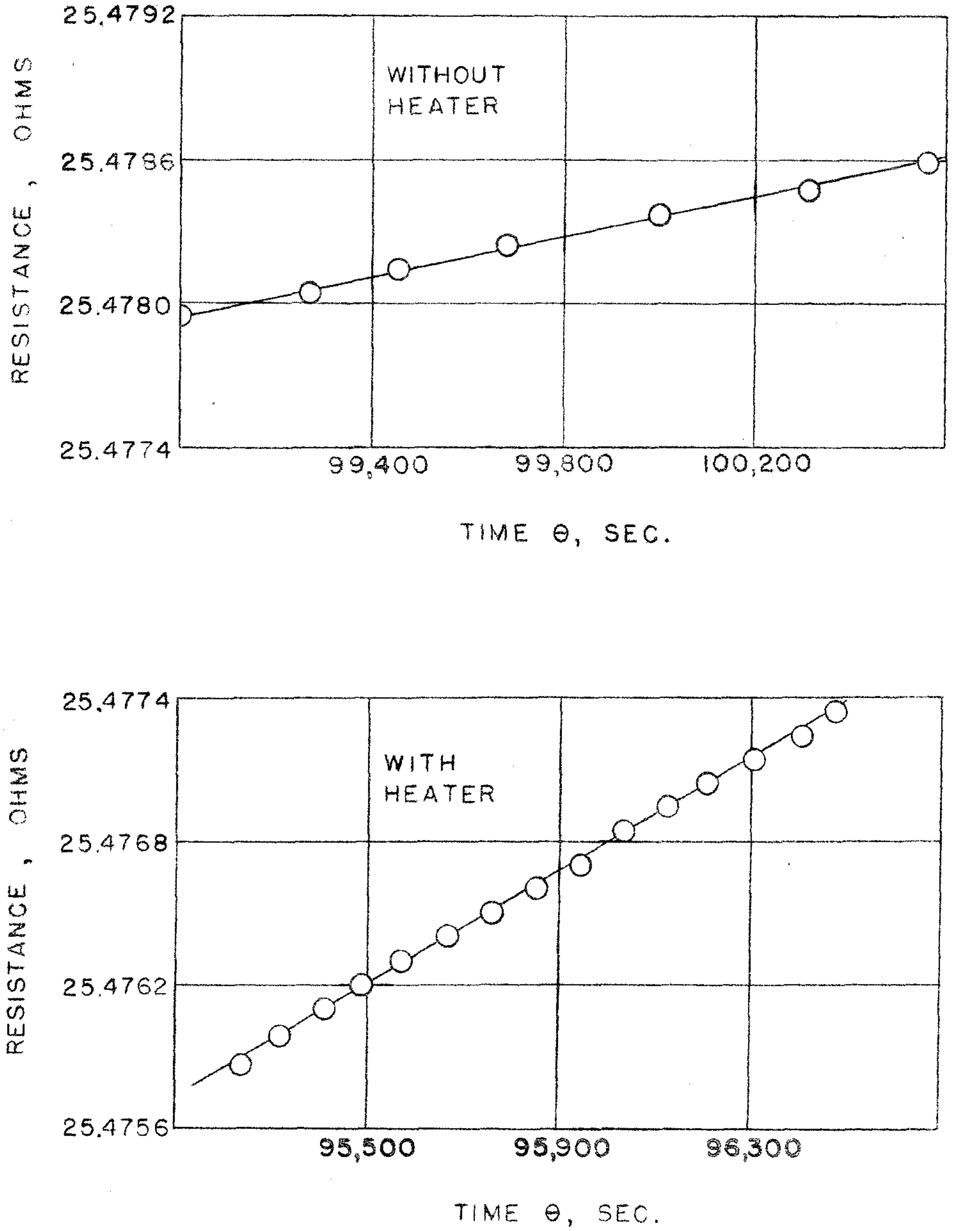

Figure 12. Calibration Curves for Agitator

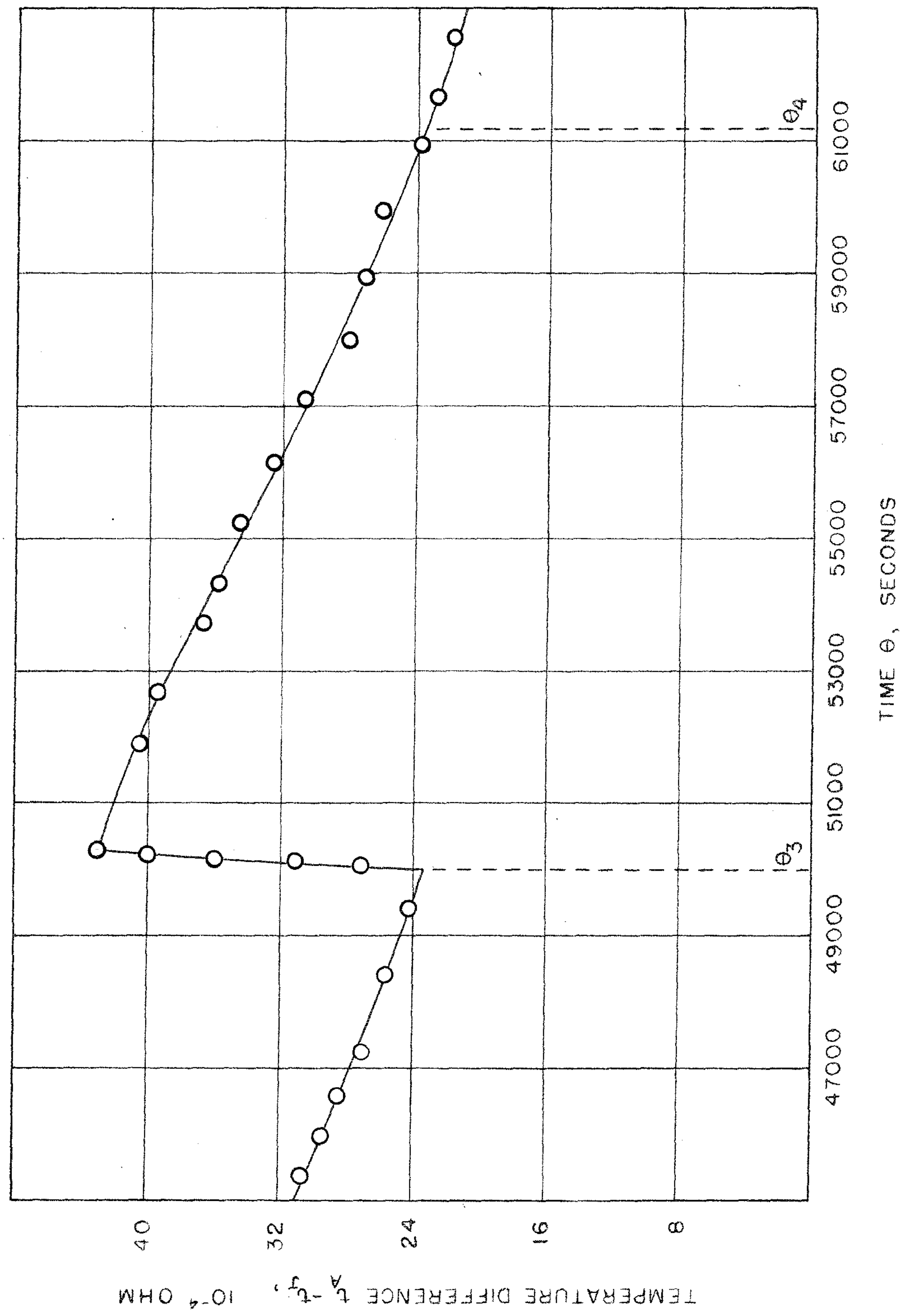

Figure 13. Cooling Curve, Heat Transfer Calibration

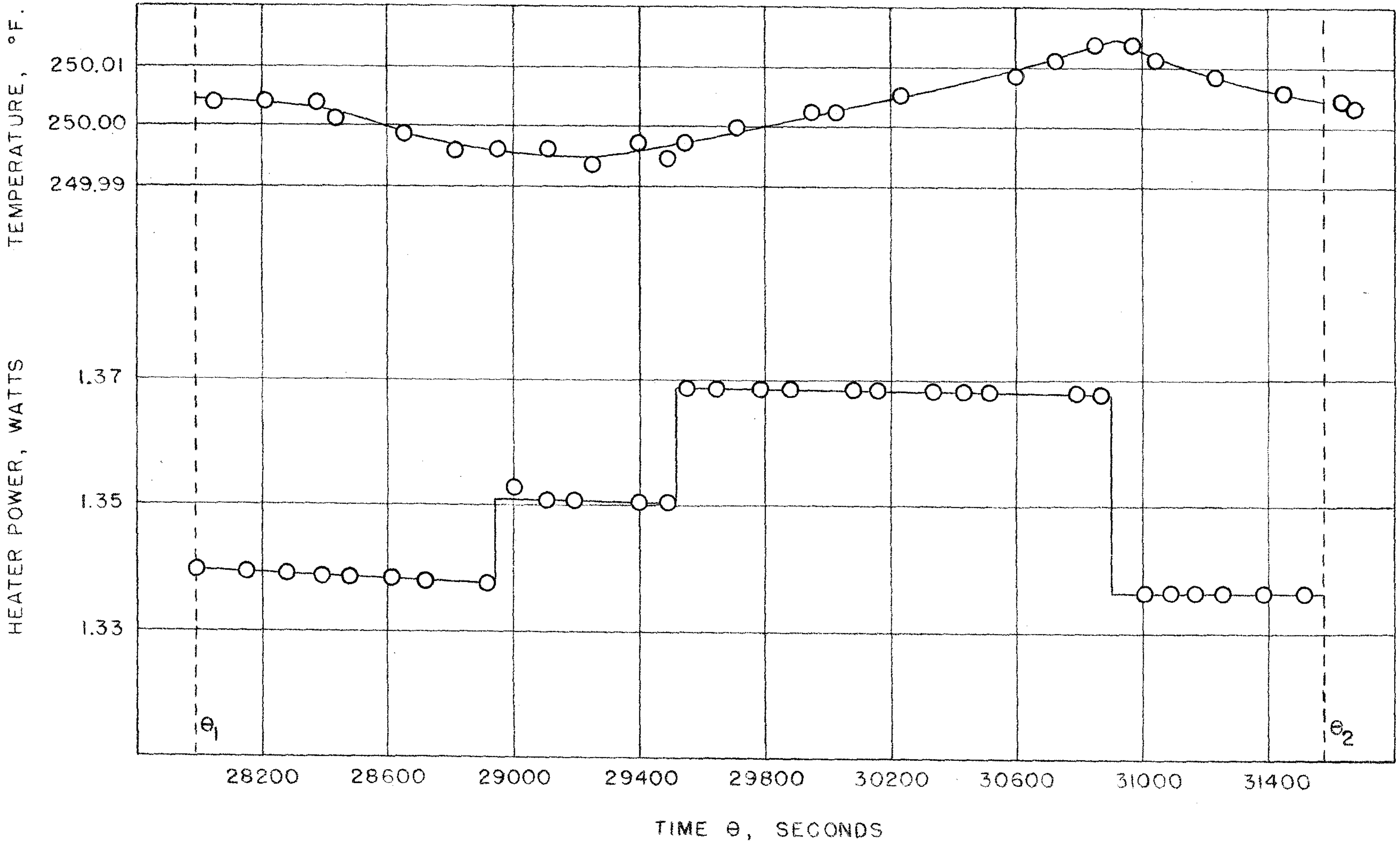

Figure 14. Temperature and Calorimeter Heater Power During Vaporization Run

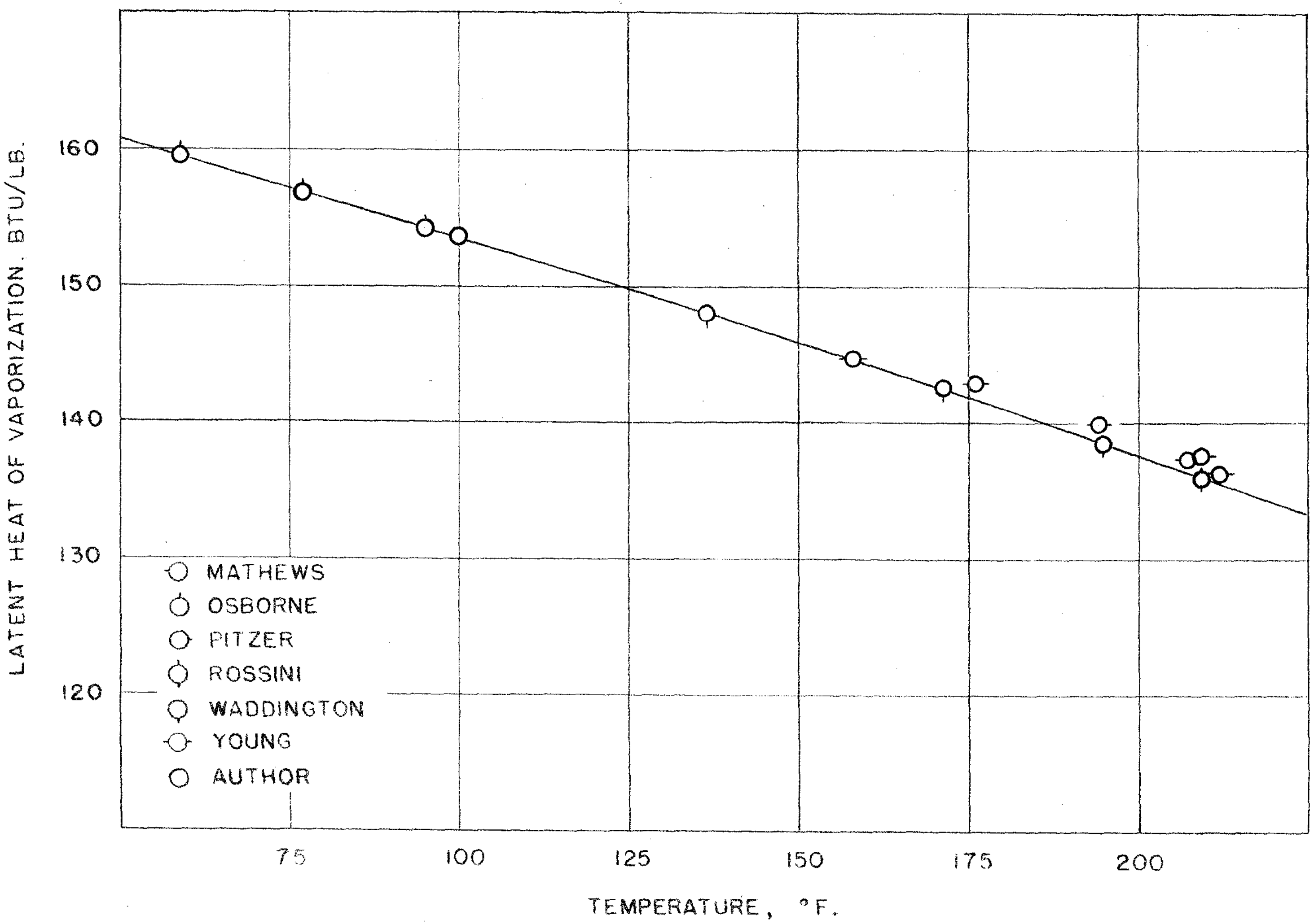

Figure 15. Latent Heat of Vaporization of n-Heptane

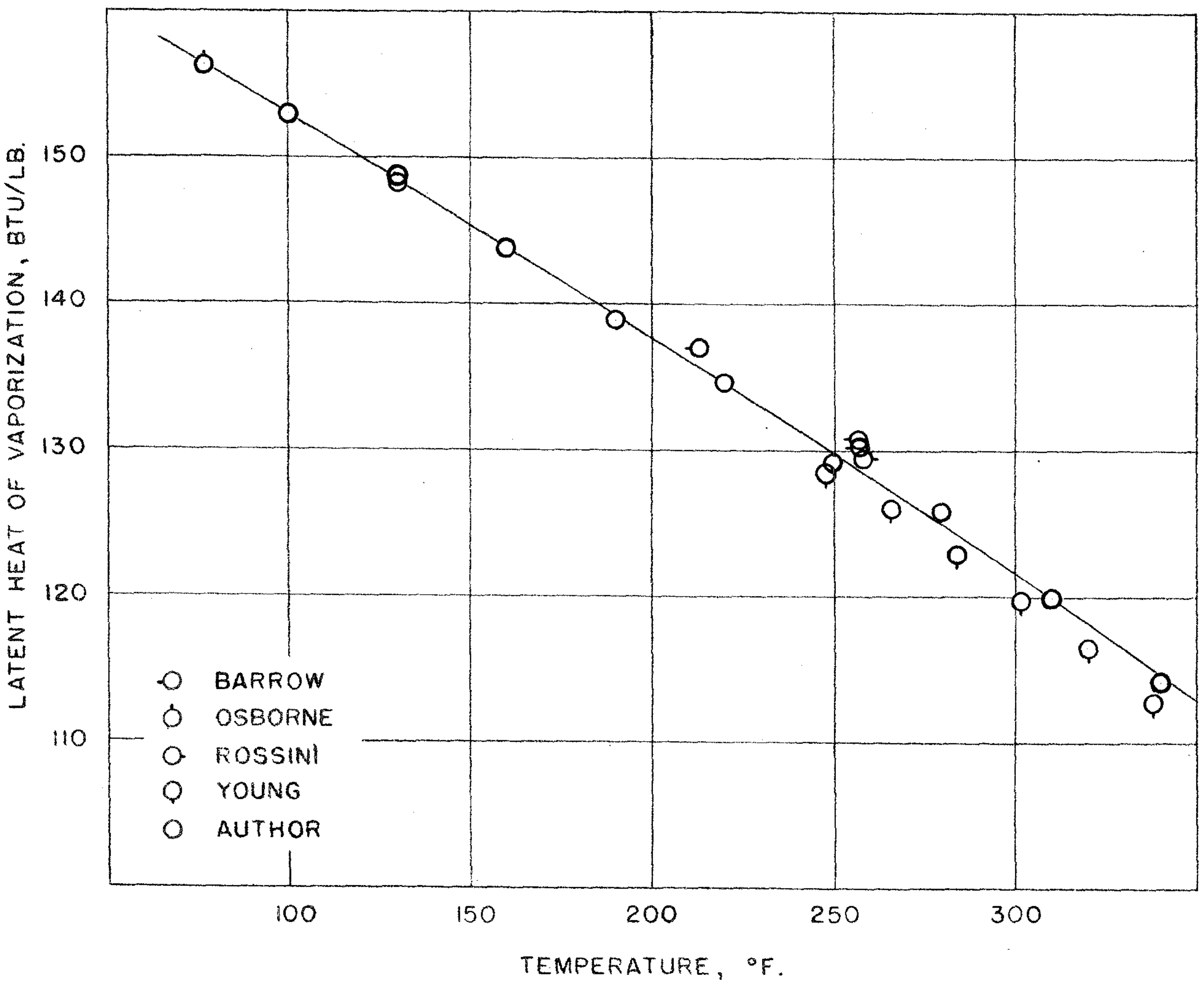

Figure 16. Latent Heat of Vaporization of n-Octane

LIST OF TABLES

TABLE I

Specific Volume of Saturated Gas, n-Octane

Temperature °F	Volume of Saturated Gas cu. ft./lb.
100	97.80
130	46.25
160	23.84
190	16.43
220	7.79
250	4.86
280	3.16
310	2.14
340	1.49

TABLE II

Latent Heat of Vaporization, n-Octane

Test No.	Temperature °F	Heat of Vaporization btu/lb (experimental)	Heat of Vaporization btu/lb (from curve)	Deviation %
197	100	152.83	152.83	0.0
199	130	148.67	148.23	+0.29
200	130	148.20	148.23	-0.02
201	160	143.71	143.71	0
202	190	138.89	139.13	-0.17
214	220	134.53	134.55	-0.01
215	220	134.48	134.55	-0.05
218	250	129.13	129.84	-0.55
219	280	125.73	125.03	+0.56
233	310	119.88	119.84	+0.03
234	340	114.05	114.32	-0.24

TABLE III

Difference in Internal Energy of Saturated Gas and Saturated Liquid, n-Octane

Temperature °F	$E_g - E_l$ Btu/lb
100	143.17
130	138.11
160	133.16
190	128.15
220	123.27
250	118.25
280	113.20
310	107.86
340	102.29

TABLE IV

Process Data, n-Octane

Test No.	t_a °F	$\theta_2-\theta_1$ sec	Electrical energy watt sec	Agitator energy watt sec	Energy transfer from surroundings watt sec	Q watt sec	m_1-m_2 grams	$(t_2-t_3)_a$ °F	Average power input Watts	Orifice diameter inches	Average rate of withdrawal gm/min
197	100.003	5826.15	5222.08	115.77	−0.81	5337.04	15.0138	0.19	0.916	0.0090 0.0198 0.0153	0.155
199	130.007	2688.22	4161.78	52.34	−0.87	4213.25	12.1842	0.21	1.567	0.0198	0.272
200	130.013	3607.50	5575.45	70.25	−2.42	5643.28	16.3717	0.21	1.564	0.0198	0.272
201	160.000	2049.52	6436.51	38.88	+0.20	6475.59	19.3779	0.43	3.159	0.0198	0.567
202	189.990	4516.98	4567.65	83.90	+2.83	4654.38	14.3908	0.15	1.030	0.0090	0.191
214	219.992	2973.01	5111.42	54.03	+1.66	5167.11	16.4731	0.25	1.738	0.0090	0.332
215	219.994	2945.04	5036.56	53.52	+1.13	5091.21	16.2372	0.25	1.729	0.0090	0.331
218	250.003	3590.65	4842.65	63.11	−0.80	4904.96	16.2543	0.21	1.366	0.006	0.272
219	279.984	2149.39	4385.05	36.49	+2.56	4424.10	15.0197	0.32	2.058	0.006	0.419
233	310.002	3547.02	3155.77	55.15	−0.63	3210.29	11.3721	0.16	0.959	0.0044	0.204
234	339.995	2362.72	3470.08	45.16	+1.10	3516.34	13.0150	0.21	1.228	0.0044	0.272

PART IA

APPENDIX

CALORIMETER HEATER CIRCUIT DETAILS

Description of Heater Circuit

The energy dissipated in the calorimeter heater was established from voltage and current measurements taken at regular time intervals during the vaporization process. A circuit diagram, Figure 1A, shows the arrangement of the equipment used for making the measurements. In some respects, the diagram is similar to the diagram of the heater circuit as originally operated (1). The important details, including the alterations which were made, are shown in Figure 1A and discussed in the succeeding paragraphs.

The calorimeter heater A, Figure 1A, includes only those parts of the heater circuit which are within the calorimeter. Current leads B carry electrical energy from the high capacity storage battery C and through the series resistor D. The current in the circuit is adjusted to a suitable value by means of the variable resistors E and M. The auxiliary heater F, of approximately the same resistance as heater A, may be used to draw current from the battery when the calorimeter heater is not in operation. This permits the circuit to reach stable operating conditions in advance of actual operation.

Current Stability and Control

The availability of a stable electrical energy supply is desirable in the present work as well as in heat capacity studies in order to make the precise measurements necessary for the evaluation of the power to the heater. The use of an auxiliary heater is unnecessary when a vaporization run or stirrer calibration is carried out since the calorimeter heater is operated during the preliminary operations for a sufficient length of time to attain stable operation prior to the period of measurement. However, when the period of measurement and the operation of the heater are started simultaneously, as in heat capacity studies or in heat loss calibrations as carried out in this work, the prior attainment of circuit stability is achieved by the use of the auxiliary heater.

The current in the circuit is determined from the voltage drop across the resistor D, Figure 1A, measured by means of the potentiometer G. Part of the current flows through the high-resistance voltage divider JK, which is connected to the current leads B at points one inch from the calorimeter by means of the potential leads ℓ. The potential drop across the heater A is determined from the voltage drop across resistor K of the voltage divider. Since the voltage drop across the resistor K is measured with the same potentiometer G, it is convenient to select the resistors D and K in such a manner that the voltage values measured with the potentiometer fall on the same part of the scale.

In heat capacity studies and vaporization studies in which the rate of withdrawal of vapor can be adjusted directly, it is customary to maintain a fixed heater setting during the period of measurement. In addition in such studies, it is possible to check the circuit for steady behavior before the period of measurement begins. However, in the vaporization studies presented in this thesis, the rate of withdrawal of vapor was fixed by the state of the fluid and the size and shape of the orifice. Consequently, the control of operating conditions within desired limits required that, during the period of measurement, adjustments be made in the calorimeter heater circuit to correct for decreasing battery voltage, changes of conditions within the calorimeter, and other changes affecting the rate of withdrawal of vapor.

It was discovered that, at the currents used in this work, unsteady operation of the heater sometimes resulted, because of an unstable contact resistance, when a single variable series resistor, such as resistor E, was used to adjust the calorimeter heater current. In addition, finer adjustment of the heater current was needed for the vaporization studies than was provided by resistor E which was installed originally for heat capacity studies. To provide the desired fine control and avoid the unsteady operation resulting from unstable contact resistance associated with the variable resistor used for control, the resistors M and P were added to the circuit, as shown in Figure 1A.

The variable resistor M, Figure 1A, is comprised of a decade box of smaller current capacity than the similar resistor E. P is of fixed resistance. The use of the shunt resistor P serves a double purpose; the current requirement through the control resistor M is decreased, and the effect of an unstable contact resistance is reduced.

The reduction in the effect due to unstable contact resistance can be illustrated simply by the following. Consider two parallel resistors, R_1 and R_2 having a combined resistance R given by

$$R = \frac{R_1 R_2}{R_1 + R_2} \tag{1A}$$

Assuming that R_2 is a variable resistor, the rate of change of R with respect to R_2 is obtained by differentiating Equation 1A with respect to R_2 ,

$$\frac{dR}{dR_2} = \frac{R_1}{R_1 + R_2} - \frac{R_1 R_2}{(R_1 + R_2)^2} \qquad (2A)$$

If the contact resistance of R_2 is represented by ΔR_2 and assuming that dR/dR_2 may be replaced by $\Delta R/\Delta R_2$, the change in the resistance of R due to the contact resistance becomes

$$\Delta R = \frac{R_1 \, \Delta R_2}{R_1 + R_2} - \frac{R_1 R_2 \, \Delta R_2}{(R_1 + R_2)^2} \qquad (3A)$$

In the course of the present investigations, the resistor E was used only for making coarse adjustments and was set and checked for good contact before the start of a period of measurement. All adjustments in the heater circuit during a vaporization run were made with the variable resistor M. Representing the resistance of the resistor M by R_2 and the resistance of P by R_1, the worst case encountered during an experiment corresponded to R_2 equal to approximately five times R_1. For this situation, it follows from Equation 3A that

$$\Delta R = \frac{1}{42} \Delta R_2 \qquad (4A)$$

Thus, the instability resulting from poor contact with the variable resistor M, used in adjusting the heater current during a run, is attenuated by the shunt resistor.

The use of better switches than those provided on the decade boxes which were used as the variable resistors in the calorimeter heater circuit would probably have eliminated the problem of erratic behavior in the circuit, although the arrangement described above provided a suitable solution using standard laboratory components.

Calculation Details

The current through the calorimeter heater A, Figure 1A, is given by

$$i_A = \frac{v_D}{r_D} - \frac{v_K}{r_K} \qquad (5A)$$

The second term in Equation 5A is the correction for the fraction of the total current in the circuit which bypasses the heater A by way of the voltage divider.

The voltage drop across heater A is given by

$$v_A = v_K \left(\frac{r_J + r_K + r_{\ell_1} + r_{\ell_2}}{r_K} \right) - 2\, r_a i_A \qquad (6A)$$

The second term in the equation represents the correction for the voltage drop across a portion of the current leads situated outside the calorimeter but within the part of the calorimeter heater circuit which is within the voltage divider loop. The resistance of this section of the leads was obtained as a function of temperature and is shown in the plot, Figure 2A. A tabulation of the resistance values of the other resistors is included in the legend to Figure 1A. The resistance values plotted in Figure 2A were calculated from the resistivity of copper, taken from the literature (20), and the dimensions of the leads.

The energy dissipated in heater A is evaluated by integration of the instantaneous power values, $i_A v_A$, over the duration of the process as follows:

$$\underline{Q}_e = \int_{\theta_1}^{\theta_2} i_A \, v_A \, d\theta \qquad (7A)$$

The resistance values r_D and r_K and the combined values $r_J + r_K$ and $r_{\ell_1} + r_{\ell_2}$ were obtained by calibration against standard resistors. If the appropriate values are substituted for the resistances in Equation 5A, there is obtained

$$i_A = \frac{v_D}{0.01001376 \text{ ohm}} - \frac{v_K}{679.069 \text{ ohm}} \tag{8A}$$

Similarly, Equation 6A becomes

$$v_A = v_K \left(15.23489\right) - 2 r_a i_A \tag{9A}$$

<u>Sample Calculation</u>

Measurements of the voltage drops v_D and v_K were obtained alternately during a period of energy evaluation. As an illustration, during a vaporization of n-octane at 250°F, the following measurements* were made:

θ = 29555 sec., v_K = 0.28105 volt

θ = 29644 sec., v_D = 0.0032016 volt

θ = 29785 sec., v_K = 0.28103 volt

θ = 29880 sec., v_D = 0.0032015 volt

By interpolation, using plots of θ vs. v_D and v_K ,

---

*These data were taken from data sheet no. 4208.02, test no. 218.

corresponding values of v_0 and v_K are obtained for each reading of time θ . Thus, at $\theta = 29644$ seconds,

$$v_0 = 0.0032016 \text{ volt, and } v_K = 0.28104 \text{ volt} .$$

For the operation at 250°F, $2r_a = 0.00595$ ohm. Therefore, the current obtained by substitution in Equation 8A is given by

$$i_A = 0.319306 \text{ amp.}$$

The voltage, from Equation 9A, is equal to

$$v_A = 4.27971 \text{ volts}$$

From these values, the corresponding power $i_A v_A$ is calculated :

$$i_A v_A = 1.36654 \text{ watts}$$

This value is plotted as one of the points on the power curve, Figure 8, presented earlier. The area under the curve represents the energy introduced by the heater, and in the example is equal to 4842.65 watt seconds. This result is listed in Table IV presented earlier.

DISCUSSION OF AGITATOR ENERGY

Calibration Procedure - General

The rate of energy addition to the calorimeter by the agitator may be evaluated by measuring the rate of rise of temperature of the calorimeter with the agitator in operation and the vapor withdrawal line closed. This rate may be compared with the rate of rise, at the same conditions, resulting from the operation of the agitator and the addition of energy by the heater at a predetermined and known rate. The comparison should be made under such conditions that the amount of energy transferred by other mechanisms, such as by conduction or radiation between the calorimeter and the surrounding jacket, is negligible or amenable to evaluation. It is desirable to be able to make the comparison for conditions of zero temperature difference between the calorimeter and the surrounding jacket. However, in practice this condition is difficult to attain, although it may be approached within reasonable proximity.

In this work, the calorimeter and the jacket were assumed to be at substantially the same temperature when the average of the top and bottom differential thermocouple readings, indicating the difference in temperature between the calorimeter and jacket walls at the top and bottom, respectively, was zero. The temperature of the calorimeter could be made to coincide with the temperature of the jacket by furnishing energy with the agitator in the final stage of the operation resulting in a rate of temperature rise of approximately 0.05°F per hour. Temperature gradients within the calorimeter, under these conditions, were assumed to be very small. However, the differential thermocouple readings in the upper and lower regions were found to differ consistently, by approximately 0.005°F, which could be attributed to parasitic voltages in some of the junctions in the associated circuits.

It may be assumed that under these conditions of apparent temperature equality, the gain or loss of energy by the calorimeter due to thermal transfer between the calorimeter and the surrounding jacket is zero. Although this assumption is reasonable, it is not necessary, since energy obtained by thermal transfer may be treated as a part of the energy introduced by the agitator. This is permissible inasmuch as the rate of transfer of energy between the calorimeter and the surrounding jacket, as discussed in the next section of the Appendix, is proportional to the temperature difference existing between them. The latter assumption implies that a departure from the conditions of temperature equality as specified above results in a change in the energy exchanged between the calorimeter and the jacket which must be considered separately.

Details of Conditions

With the jacket surrounding the calorimeter maintained at a constant temperature, the temperature of the calorimeter was observed as a function of time, first with just the agitator in operation and subsequently with both the heater and the agitator in operation. In the latter case, the contribution by the heater was approximately the same as by the agitator. The temperature range of the calorimeter extended from approximately 0.04°F below to approximately 0.04°F above the temperature of the surrounding jacket in both cases. The results were plotted, as shown in Figure 12, and slopes were determined graphically giving the rate of rise of temperature of the calorimeter for the conditions described above.

Evaluation of Agitator Power

The rate of energy addition by the agitator, $\mathcal{P}_s$, is determined by the following expression

$$\mathcal{P}_s = \frac{S_1}{S_2 - S_1} \mathcal{P}_e \qquad (10A)$$

where S_1 is the rate of rise of temperature resulting from the operation of the agitator, S_2 is that due to the operation of the agitator and heater combined, and P_e is the rate of electrical energy addition to the heater.

Practical Limitations

In practice it was difficult to determine the slopes S_1 and S_2 accurately since the temperature changes involved in the calibration procedure were not large in comparison with the precision of the temperature measurements. Moreover, as pointed out previously in this thesis, the motor used for driving the agitator was undersized and gave considerable trouble. Although the motor was of a synchronous type, evidence of random slipping was occasionally encountered. A constant speed of rotation of the agitator is important since the energy supplied by the agitator is proportional to approximately the cube of the speed.

Treatment of Experimental Results

In the work carried out with n-heptane, the rate of energy addition by the agitator was evaluated by means of Equation 10A from the slopes S_1 and S_2 determined at 100°F and a knowledge of the electrical power supplied by the heater. For n-octane, values of S_1 and S_2 were determined as functions of temperature over the range of interest. In the agitator calibrations the rate at which energy was added electrically was substantially constant at values from 0.0291 to 0.0306 watt. This required that the values of S_2 be adjusted to correspond to the same value of P_e (0.0296 watt) in order that a comparison of the results could be made. The adjusted values, designated by S_2', were obtained from the following equation.

$$S_2' = (S_2 - S_1)\frac{P_e}{0.0296 \text{ watt}} + S_1 \tag{11A}$$

Thus, that part of the slope S_2 resulting from the operation of the heater was scaled in proportion to the heater power. The values of S_1 and the adjusted values S_2' are plotted as functions of temperature in Figure 3A.

Results and Application

The energy addition rate due to the agitator, evaluated by means of Equation 11A, was obtained for n-octane by the use of slopes established from Figure 3A and a heater power value of 0.0296 watt. The values of P_s obtained with n-octane are given in Table IA and correspond to weights of n-octane in the calorimeter approximately in the range from 540 to 610 grams.

Since the rate of energy contributed by the agitator was assumed to be constant during a vaporization run at a particular set of operating conditions and independent of the change in the amount of material within the calorimeter, the energy added by the agitator during a vaporization run is given by

$$\underline{Q}_s = P_s \left(\theta_2 - \theta_1\right) \qquad (12A)$$

As an illustration, in a vaporization of n-octane at 250°F the duration of the run was 3590.7 seconds (Test no. 218), and the value of P_s , given in Table IA, was 0.0176 watt. The use of Equation 12A yields

$$\underline{Q}_s = 0.0176 \text{ watt} \times 3590.7 \text{ seconds}$$

or

$$\underline{Q}_s = 63.20 \text{ watt seconds} \quad \text{(Test no. 218)}$$

Discussion

Greater accuracy in calibrating the agitator could be attained by the installation of a suitable drive motor and by improving the precision in the measurement of small temperature changes within the calorimeter. A replacement motor of adequate size has been purchased; improvement in the precision of the temperature measurement is less readily achieved.

An improvement in the determination of the rate of rise of the temperature of the calorimeter due to the operation of the agitator as well as in the case of the operation of the agitator and the heater could be obtained by matching the temperature of the calorimeter and of the surrounding jacket throughout the determination. Larger temperature rises could thus be treated, decreasing the need for greater precision in temperature measurement.

Since the largest known source of error in the present work is introduced in the calibration of the agitator, an improvement in the accuracy of the calibration would be most beneficial. Operation of the agitator at a lower speed would reduce the need for accuracy in the calibration by reducing the fraction of the total energy contributed by the agitator. However, the present speed (approximately 32 revolutions per minute) represents a reasonable compromise between a high speed resulting in a more uniform temperature within the calorimeter and a low speed desired for reasons of calibration.

DISCUSSION OF HEAT LOSS

In Part I of this thesis, under the section on Energy Calculations, it was shown that the rate of energy exchange by conduction and radiation between the calorimeter and the surrounding jacket may be considered proportional to the temperature difference between the calorimeter and the jacket when the difference is small. Therefore, repeating Equation 26 here for convenience, the energy so transferred is

$$Q_J = \int_{\theta_1}^{\theta_2} k\left(T_J - T_A\right) d\theta \qquad (13A)$$

The relation between the temperature difference and the resultant transfer of energy involved may be estimated by at least three methods.

Method One

The first method consists in maintaining the surrounding jacket at a constant temperature and permitting the calorimeter to reach thermal equilibrium while operating the calorimeter heater at a small, constant rate P_e . When thermal equilibrium is attained, the rate of energy transfer from the calorimeter equals the power input to the heater and may be related to the observed temperature difference between the calorimeter and the surrounding jacket. Rearranging Equation 13A, in the differential form, and substituting the heater power for the rate of energy transfer, the following result is obtained.

$$k = \frac{q_J}{d\theta} \frac{1}{T_J - T_A} = P_e \frac{1}{T_J - T_A} \qquad (14A)$$

Although this procedure is simple, it has the disadvantage of being very time-consuming due to the slow rate at which the temperature equilibrium is reached. Moreover, on account of the small temperature differences desired in the calibration, a drift in the electrical power supplied to the heater shifts the thermal equilibrium of the calorimeter significantly so that a very stable power supply is needed.

Method Two

In the second method, the relation between the temperature difference $T_J - T_A$ and the resultant energy transfer may be determined from the cooling curves obtained when the calorimeter and contents are allowed to cool while the temperature of the jacket is held constant. To apply this method, a knowledge of the heat capacity of the calorimeter and contents is necessary since the quantity $q_J/d\theta$, used in evaluating the proportionality constant k in Equation 14A, is calculated by taking the product of the heat capacity and the slope of the cooling curve. The slope of the cooling curve is difficult to obtain with good accuracy in the region of small temperature differences owing to the limitations imposed by the precision of temperature measurement.

Method Three

The third method involves heating the calorimeter above the temperature of its surroundings by investing a measured amount of energy and observing the temperature-time path by which the calorimeter returns to the initial temperature. The desired results are evaluated by means of Equation 13A, rewritten in the following form

$$k = \frac{\underline{Q}_J}{\int (T_J - T_A)\, d\theta} \qquad (15A)$$

where the energy $\underline{Q}_J$, lost by the calorimeter, equals the measured input of energy. The input of energy is introduced by the heater and agitator and is evaluated as described previously.

If, in the third method, the calorimeter is heated when it is at the temperature of the jacket and then allowed to cool to the jacket temperature, the calibration becomes very time consuming owing to the slow rate of attainment of thermal equalibrium under these conditions. In addition, the evaluation of the area under the cooling curve (the integral, Equation 15A) is subject to relatively large uncertainties in the region where the temperature difference approaches zero. Therefore, it is advisable to introduce heat to the calorimeter at a point where the temperature difference on the cooling curve is greater than zero, and then to cool again to the same temperature. Such a path is shown in Figure 7 presented earlier.

The Calibration

The first and third methods discussed above are believed to be more accurate than the second for heat loss calibration. The third method was employed in this work because it was believed to be quicker than the first and of comparable accuracy.

Calibrations were carried out to give the proportionality constant k , in Equation 13A, at 130 and 310°F. Values of k at other temperatures of interest were obtained by linear extrapolation and interpolation of the values obtained experimentally, as shown in Figure 4A. The results are listed in Table IIA in the units which were most convenient in this work (watt sec./ohm sec.).

Heat Loss Calculation

The energy transfer between the calorimeter and the vacuum jacket involved during a vaporization run was evaluated by the application of Equation 14A over the duration of the process. As an illustration, the curve, Figure 8, presented earlier, represents the process variables of interest during Test no. 218, giving the temperature difference $T_J - T_A$ as a function of time. The area under the curve is 0.415 ohm second and represents the value of the integral, Equation 14A, for this test carried out at 250°F. The product of this area and the value of k given in Table IIA yields

$$\underline{Q}_J = + 0.80 \text{ watt sec. (Test no. 218)}$$

This result is included in Table IV.

Discussion

It should be recognized that the temperature distribution during a vaporization run is different from that obtained during a calibration for k . Consequently, the k obtained by calibration is actually an approximation. However, the average temperature of the calorimeter is assumed to be the temperature of the liquid phase, which occupies two to three times the volume of the gas phase. The conduction of heat from the jacket to the top of the calorimeter, along the vapor-withdrawal tube, is prevented by the flow of the vapor. The temperature gradient along the tube carrying the thermometer leads, which is measurable, was found to be insignificant. Thus it is believed that the value for k obtained by calibration is valid.

DETAILED DESCRIPTION OF APPARATUS

The apparatus, modified in this work for the purpose of extending its utility to include the measurement of latent heats of vaporization, is described in its original form in the literature (1). For the convenience of the reader interested in the details of the apparatus assembly and for the purpose of completeness, a detailed description is presented here which includes the changes and the additions made to the original apparatus as well as including a description of those parts which are unchanged and also described in the above reference. This description supplements that given earlier in this thesis.

The Calorimeter Assembly

The general arrangement of the calorimeter assembly is shown in Figure 2, presented earlier. The calorimeter A, comprised of two parts, was machined from type 302 stainless steel. The two parts were joined by means of a tapered Acme thread which provided the required strength with the minimum of additional metal. Pure tin was used to provide a pressure-tight seal within the threads. The vessel was designed to operate at pressures up to 1000 pounds per square inch, resulting in a maximum stress in the steel of 20,000 pounds per square inch. The calorimeter was supported from the jacket J by means of three small wires which were fastened to lugs in the top part of the calorimeter. Two lugs in the bottom part of the calorimeter serve to reinforce the walls where the heater leads leave the calorimeter. The lugs were useful in the assembly and disassembly of the calorimeter. The two parts of the calorimeter are shown before assembly in the photograph, Figure 5A. A portion of the thermometer well used in the earlier work is shown with the top part. Within the bottom part the supports for other internal parts of the calorimeter may be seen. The outer surface of the calorimeter and the inner surface of the vacuum jacket were polished to reduce transfer of energy by radiation between the two surfaces.

The centrifugal agitator B, Figure 2, provides stirring of the fluid within the calorimeter. The liquid leaving the agitator flows through the ports C in the shield D, upward through the passage between the shield and the inner wall of the calorimeter A, past the heater (not shown in Figure 2), down past the well enclosing the resistance thermometer E, and back to the agitator along the radial guide vanes F. The heating element is enclosed within 1/8 inch-diameter steel tubing coiled to resemble a helix of 7-1/2 turns on a diameter of 4-5/8 inches. The heater is situated in the annular space between the circulation shield and the inner wall of the calorimeter and extends from a point just above the ports C to a point slightly below the mid-point of the calorimeter. The circulation of liquid samples of the amount just sufficient to cover the heater was made possible by cutting additional ports (not shown in Figure 2) in the shield D. The additional ports, and the arrangement of the heater as described here, made it possible to increase the permissible variation in the volume of sample within the calorimeter by a factor of ten in comparison with the original assembly. A small portion of the liquid pumped by the agitator B through the ports C flows downward into the region within the calorimeter below the agitator and then upward through holes located near the eye of the agitator. The shield and radial guide vanes, parts of the agitator, and the support for the shield, are shown in the photograph, Figure 6A. The additional ports which were cut in the shield are not shown.

The agitator is supported by steel and bronze bearings, shown in Figure 2, and is driven by the shaft G. The tube H, which encloses the shaft, is connected to the calorimeter at the lowest point and leaves the vacuum jacket through the seal I located in the sleeve U. The sleeve U is an extension of the vacuum jacket and serves to lengthen the path of direct contact between the calorimeter and its surroundings at the lower end of the calorimeter. Along this path the tube is thin-walled. Two small ports (not shown in Figure 2), provide openings between the lowest points within the calorimeter and the annular space between the shaft G and the interior of the tube H. One of these ports may be seen in the photograph, Figure 5A. These passages are used in the operations of loading and unloading the calorimeter. The shaft G, the tube H, and all of the parts within the calorimeter with the exception of the bronze bearings are stainless steel.

The original well which contained the resistance thermometer E, Figure 2, was open to the vacuum chamber and consequently the thermometer was maintained in a vacuum during operation. The replacement well, shown earlier in the drawing, Figure 3, and in the photograph, Figure 4, permits operation with the thermometer in a gaseous atmosphere (of helium), resulting in improved response of the thermometer. The replacement also provides a port for the removal of vapor from the top of the calorimeter. The vapor line and the tube which carries the thermometer leads from the top of the calorimeter are shown in the photograph, Figure 5, and are described in detail earlier in this thesis in the Description of Apparatus section. The tubes leave the chamber within the vacuum jacket by way of the vacuum line which is not shown in Figure 2 but which may be seen in the above photograph. A thin shield of aluminum is supported by the tubes in the region between the calorimeter and the vacuum line to provide a barrier to radiation from the calorimeter through the vacuum line. In the absence of a shield, a portion of the calorimeter would radiate directly to a water-cooled surface.

The Oil Bath

The vacuum jacket J, which was machined from stainless steel, is surrounded by the oil bath K, Figure 2. Circulation within the oil bath is provided by the impeller L which pumps oil through the ports M, up and around the circulation shield N and past two heaters of helical design which are situated in the annular enclosure between the shield N and the bath K. The oil bath with the impeller installed is shown in the partial assembly, Figure 7A. The brackets which support the heaters may be seen in the photograph, Figure 8A. The oil then flows through the openings O in the circulation shield, Figure 2, downward past a resistance thermometer (not shown), along the vacuum jacket, past the radial guide vanes R, through the ports S and downward past the circulation shield T which turns with the impeller. The flow is then inward toward tube H, upward past sleeve U, and back into the impeller.

The impeller is driven by the sleeve V which in turn is driven by the sleeve W. The sleeve W, which rotates within the bearing A', leaves the oil bath through the packing gland X. The pulley B', supported by the bearings C' and D', drives the sleeve W through a coupling located just below the packing gland Y. The bearing Z provides support for the sleeves V and W. The impeller and auxiliary parts, partially assembled, are shown in the photograph, Figure 9A. The exterior of the oil bath with the impeller drive installed is shown in the photograph, Figure 10A.

In the operation of the calorimeter during heat capacity studies, a defect in the coupling by which sleeve W was driven caused the assembly of sleeves V and W and the impeller L to move upward. This caused the impeller to rub on the radial vanes P. As a result, metal particles were formed which lodged within the bearing A' and the packing gland X and caused severe scoring of the surfaces involved. The defect in the coupling was corrected, new bearing surfaces were machined on sleeve W, and the sleeve of bearing A' was re-designed to prevent the migration of solid particles between the rubbing surfaces.

The steel from which the jacket J was machined was found to contain non-metallic inclusions which permitted a minute flow of oil into the vacuum chamber within the jacket. It is believed that the oil thus introduced was responsible for the failures experienced in the previous work in obtaining good thermal insulation of the calorimeter and maintaining a good vacuum within the jacket. These flaws in the jacket were repaired with the result that in the present work an excellent vacuum and good thermal insulation of the calorimeter were achieved and maintained.

Agitator Drive

The tube H, which encloses the drive shaft for the agitator B is sealed to the steel shell E' just below the nut F'. The armature housing G' is suspended by means of the drive shaft G and rotates between the small steel and bronze bearings located at I' and J'. The bearing at I' is a combination journal and thrust bearing. The parts of the apparatus were so proportioned that at the time of assembly, the armature housing could be suspended vertically approximately midway within the space within the steel shell E' such that the thrust bearing at I' had a gap of approximately 0.025 inch. Consequently it is expected that the bearing supporting the agitator within the calorimeter should wear approximately 0.025 inch before the thrust bearing at I' gives support to the armature. The support bearing within the calorimeter was made oversized by this amount. This arrangement was used to extend the total life of the bearings and to insure that the shaft G was under tension to minimize whip.

Torque for turning the agitator is transmitted to the armature H' by means of the rotating electromagnets K' which are energized through the slip rings L' and M'. The electromagnet assembly is supported by bearings at O' and N' and is driven by the pulley P'. The details of the electromagnetic drive are shown in the photograph, Figure IIA. The electromagnetic drive provides sufficient torque to drive the agitator at speeds up to 200 revolutions per minute. The original drives for the impeller and agitator are shown in Figure 12A.

Arrangement for Pressure Measurement

The tube which leaves the bottom of the steel shell E', Figure 2, may be used for transferring material to or from the calorimeter. This tube and the tube H are connected to the free space within the steel shell through small ports (not shown in Figure 2), which bypass the bearings at I' and J'. The pressure within the tube from the bottom of the shell may be transmitted to a pressure balance (13) through a steel diaphragm (not shown). The diaphragm prevents the mixing of the oil used in the pressure balance with the material being investigated. The control of the position of the diaphragm, indicated by an electric contact, is important in the calibration and use of the pressure-measuring system. The diaphragm was stretched during the previous operations but the subsequent satisfactory relationship between pressure difference across the diaphragm and displacement is shown by the curve, Figure 13A. The methods of calibration and the principles of operation associated with the pressure measurement are described in the literature (13). The accuracy of the pressure measurements by this method is within 0.2 per cent or 0.2 pounds per square inch, whichever is larger.

Adiabatic Jacket

The oil bath K, Figure 2, is surrounded by an adiabatic jacket which is not shown in this figure. The two sections of the jacket are shown in the photograph, Figure 14A, and the lower section may be seen in its final position in the photograph, Figure 6. Heaters with a manual control are provided so that the adiabatic jacket may be maintained at a temperature nearly equal to that of the oil bath. This provision makes it possible to maintain the oil bath at the desired temperature with only small additions of energy, thus permitting the fine temperature control needed in this work.

General Layout

The general arrangement of the calorimeter and some of the control equipment is shown schematically in Figure 15A and in a perspective view in Figure 16A. A housing unit, separately ventilated and consisting of two small rooms, was used to enclose the calorimeter and auxiliary equipment as a safety feature in the event of failure of the calorimeter during the studies conducted with corrosive materials. The structure of the housing unit is of steel. The inner and outer walls of the room containing the calorimeter are constructed of transite sheeting. The oil bath A, Figure 16A, is located within the calorimeter room B. The drive mechanisms for the calorimeter agitator and the oil bath impeller are situated near C below the bench E. The adiabatic jacket D and the other shields which surround the calorimeter are supported above the bench by supports which are shown in Figure 10A. The orifice block and the weighing-bomb condensers, described earlier, are shown in the photographs, Figures 9, 10, and 11 and schematically in Figure 15A.

Auxiliary Equipment

The second small room F, Figure 16A, serves to house most of the auxiliary equipment. The mechanical vacuum pump G in series with the three-stage jet pump H is used to evacuate the chamber around the calorimeter within the vacuum jacket. In the heat capacity studies carried out previously with this equipment, the potentiometer I (Leeds and Northrup Student type) was used in conjunction with a differential thermocouple, the galvanometer J, the photoelectric circuit K, the light source L, and one of the heaters within the oil bath, to control the temperature of the oil bath. These controls were used for the purpose of maintaining a very small temperature difference between the calorimeter and the surrounding jacket as the calorimeter was heated. The photoelectric circuit K and the corresponding control panel P were not used in the present work. In the measurement of latent heats of vaporization, the oil bath is maintained at a constant temperature by controls located in another room, and the potentiometer I is used to measure temperature differences between the calorimeter and points along the vapor-withdrawal path. Deflections of the galvanometer J, used in conjunction with the potentiometer, are observed as displacements of a light beam on the ground glass scale O, originating from the light source M, reflected by the galvanometer mirror, the mirror N, and another mirror not shown. The controls for the potentiometer I are located on panel Q.

The Leeds and Northrup type K-2 potentiometer R, Figure 16A, is used to obtain the current through and the voltage across the calorimeter heater. Controls for the heater are located above the galvanometer J and on the panel S. The controls for the type K-2 potentiometer are located on panels Q and S. The deflections of the galvanometer used with this potentiometer are observed on the ground glass scale T which receives a light beam from the light source U, reflected by the galvanometer mirror, the mirror V, and another mirror not shown. Controls for immersion and external heaters for the oil bath are located on panel X. These heaters are used in the preliminary operations of adjusting the oil bath to the desired operating temperature.

In the present work, a mechanical pump, a jet pump, and auxiliary equipment, located near W, Figure 16A, were installed and are used to evacuate the calorimeter and associated lines. This vacuum equipment is shown in the photograph, Figure 17A. A view of the interior of the control room is shown in the photograph, Figure 18A, taken before the installation of this vacuum equipment and some of the other auxiliary equipment used in the present work. The control panels of Figure 16A are shown in the photograph, Figure 19A. Additional controls mounted below the bench in Figure 19A are shown in the photograph, Figure 20A. The top item in Figure 20A controls a transformer which supplies power for heating the adiabatic jacket. The other items are controls for transformers which supply power used in heating the parts of the apparatus which convey vapor withdrawn from the calorimeter to the orifice which regulates the flowrate. These latter transformers are used in conjunction with the group of isolation transformers shown in the photograph, Figure 21A.

Additional Equipment

Additional controls and instruments used with the calorimeter are located in another room and are shown in the photograph, Figure 22A. These include the two Mueller bridges used in measuring the temperatures of the calorimeter and the oil bath, respectively, a K-2 potentiometer, used in measuring the temperature difference between the adiabatic jacket and the oil bath, and the White double-potentiometer, used in measuring temperature differences between the calorimeter and the surrounding jacket. The White potentiometer is also used to measure temperature gradients along the two tubes which leave the top of the calorimeter, the gradient along one of the current leads to the calorimeter heater, and the gradient within the thermometer well within the calorimeter. The electronic modulating circuit used in conjunction with one of the Mueller bridges to control the temperature of the oil bath is not shown, although the associated controls may be seen on the panel above the bridges, Figure 22A.

Ease of communication between the two operators located at the two control stations shown in Figures 18A and 22A is very important for the successful operation of this equipment. A commercially-available intercommunication system with the components located at the two control stations, was installed for this purpose.

LIST OF FIGURES (APPENDIX)

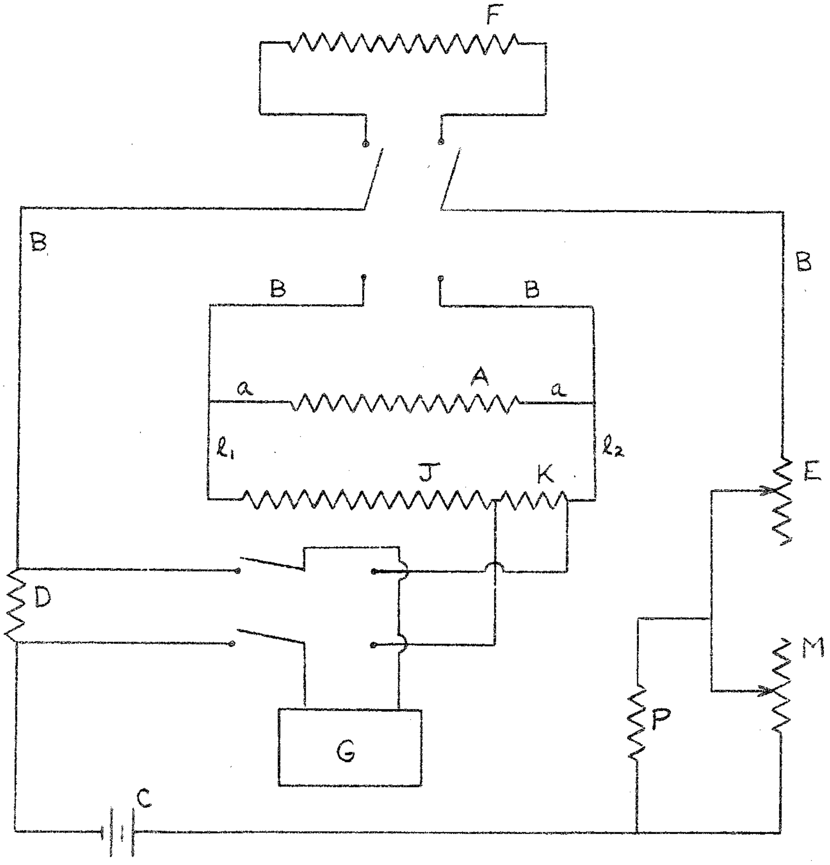

$$i_A = \frac{v_D}{r_D} - \frac{v_K}{r_K}$$

$$v_A = v_K\left(\frac{r_J + r_K + r_{l_1} + r_{l_2}}{r_K}\right) - 2\, i_A\, r_a$$

$$Q_e = \int_{\theta_1}^{\theta_2} i_A\, v_A \; d\theta$$

Figure 1A. Circuit Diagram, Calorimeter Heater

NOMENCLATURE - FIGURE 1A

A	calorimeter heater
a	part of current leads
B	current leads
C	batteries
D	resistor for measuring current in circuit
E	variable resistor for coarse control
F	auxiliary heater
G	potentiometer
i	current
JK	voltage divider
ℓ	leads in voltage divider loop
M	variable resistor for fine control
P	shunt resistor
$\underline{Q}_e$	energy (electrical)
r	resistance
v	voltage

CIRCUIT VALUES - FIGURE 1A

v_C	12 volts
r_D	0.01001376 abs. ohm
r_E	0, 1, 2, . . . 19, 20, or 240 ohms
$r_J + r_K$	10,344 abs. ohms
r_K	679.07 abs. ohms
$r_{\ell_1} + r_{\ell_2}$	1.41 ohms
r_M	40, 41, 42, . . . 48, 49 ohms
r_P	10 ohms
$2r_a$	See Figure 2A

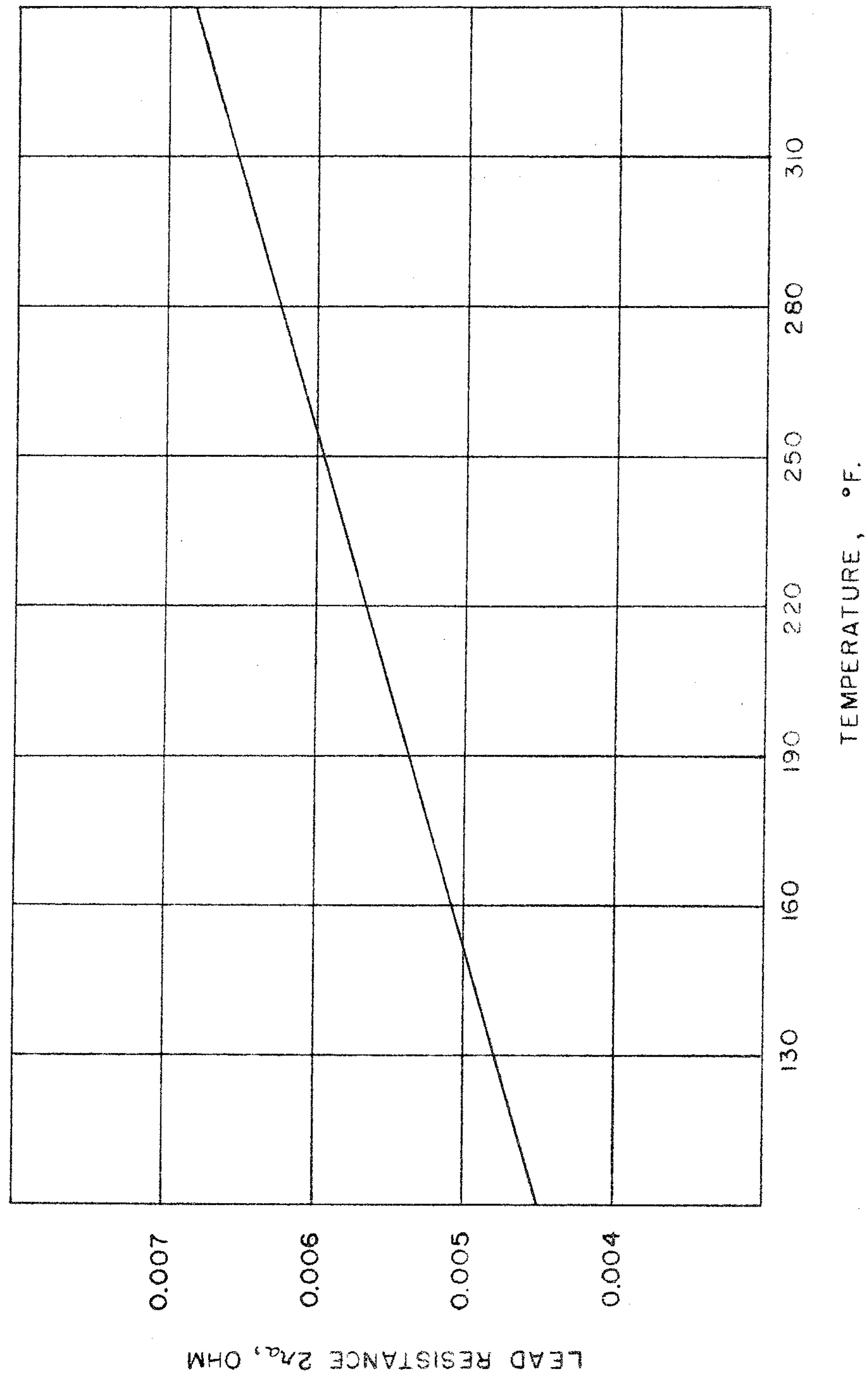

Figure 2A. Lead Resistance $2r_a$ vs. Temperature

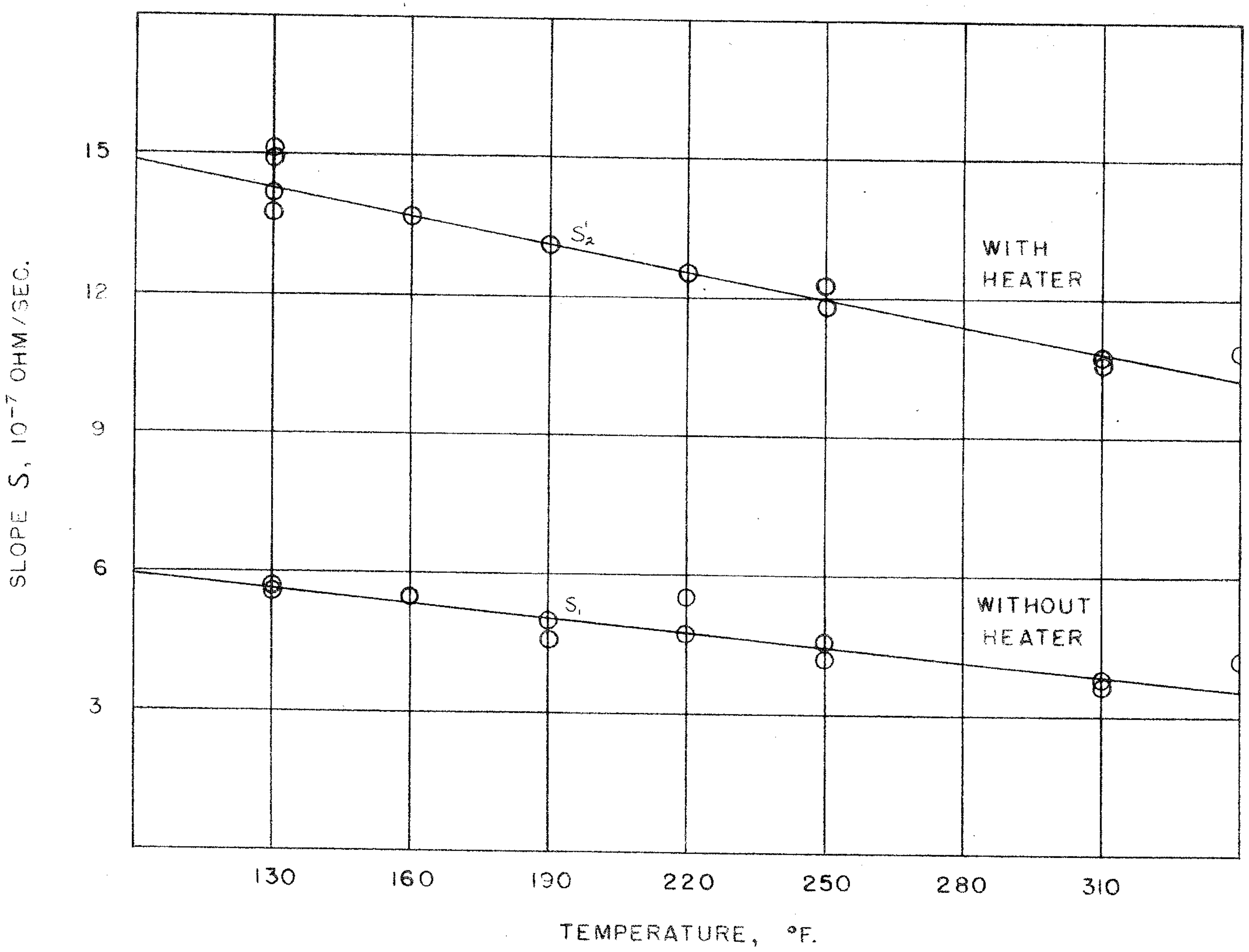

Figure 3A. Calibration Curves for Agitator

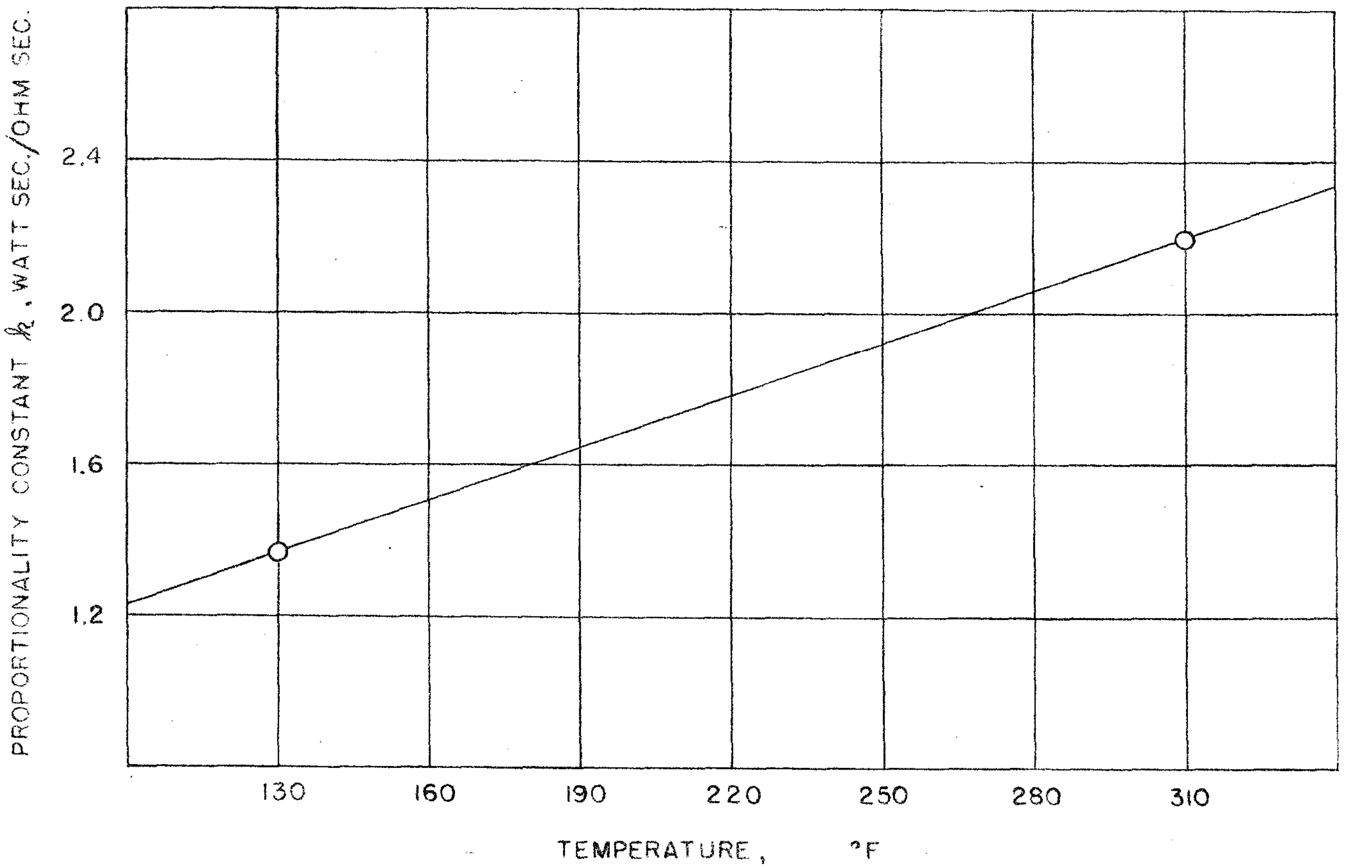

Figure 4A. Proportionality Constant k vs. Temperature

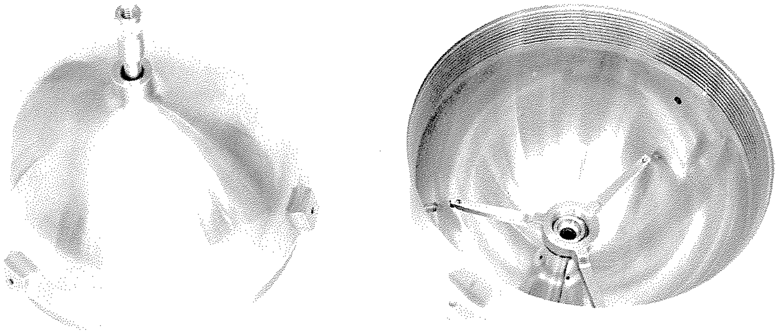

Figure 5A. Calorimeter Before Assembly

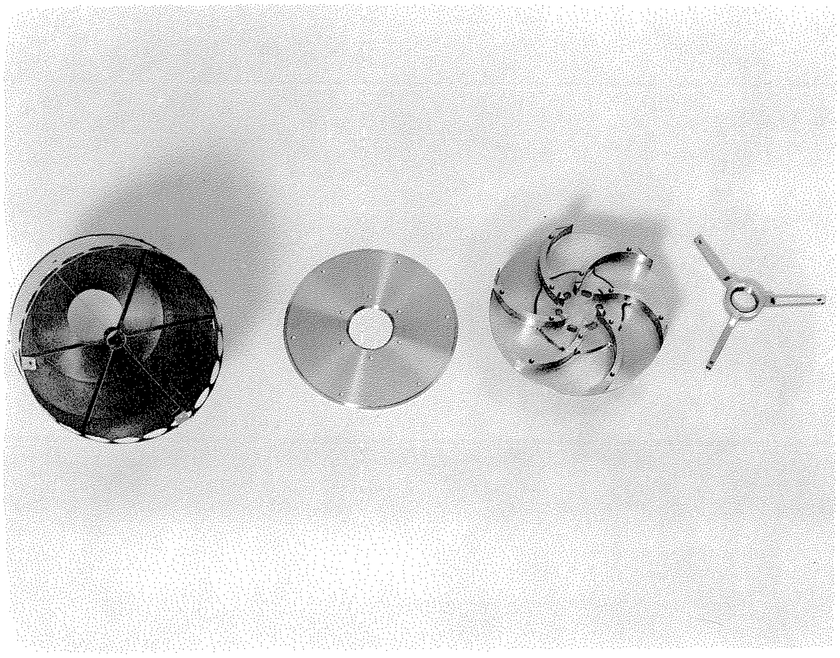

Figure 6A. Internal Parts of Calorimeter

Figure 7A. Oil Bath with Impeller, Partially Assembled

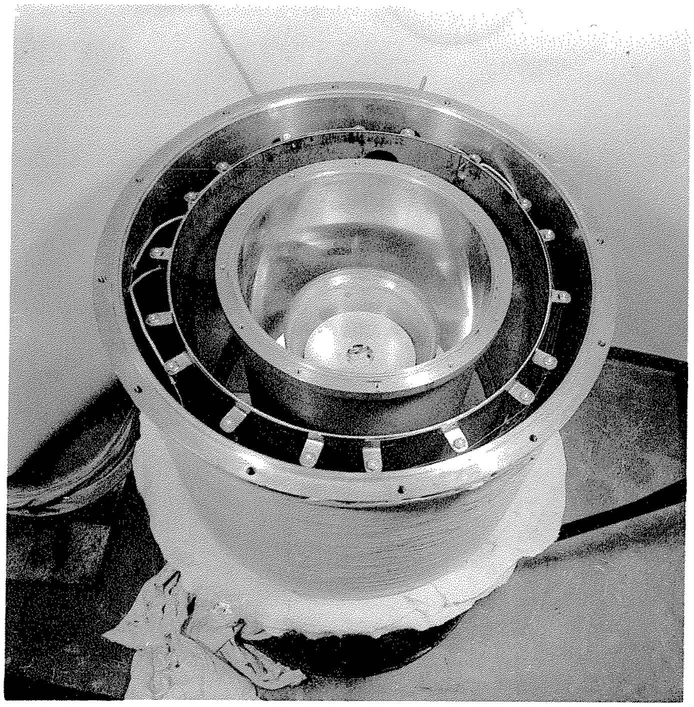

Figure 8A. Calorimeter, Vacuum Jacket, and Oil Bath,
Partially Assembled

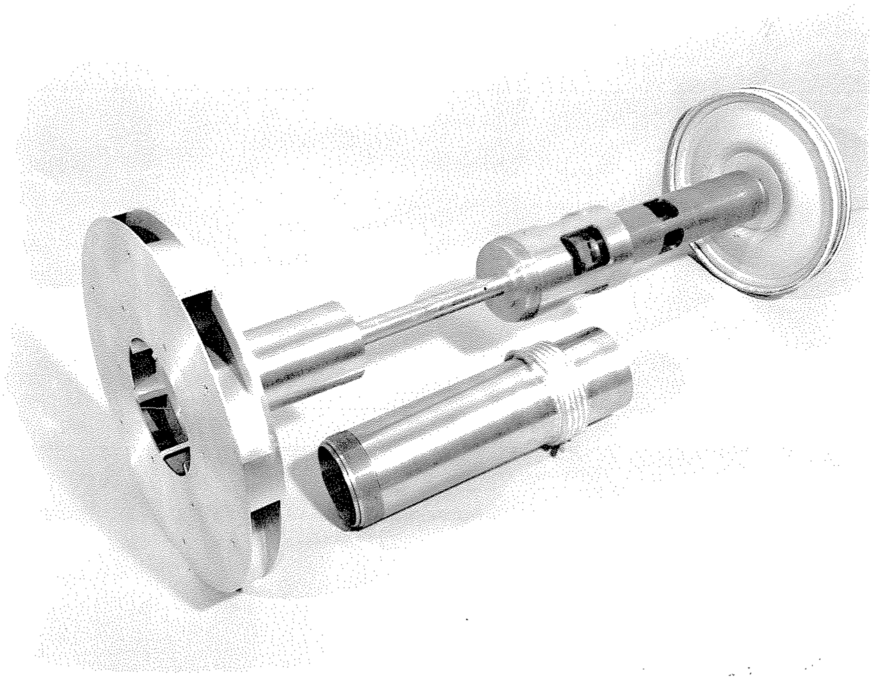

Figure 9A. Impeller and Auxiliary Parts, Partially Assembled

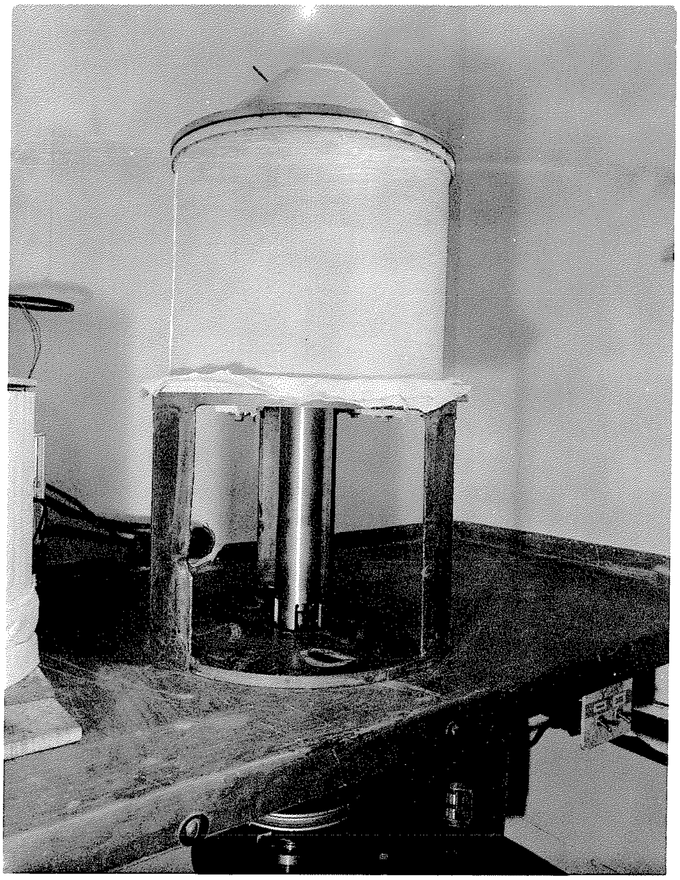

Figure 10A. Exterior of Oil Bath with Impeller Installed

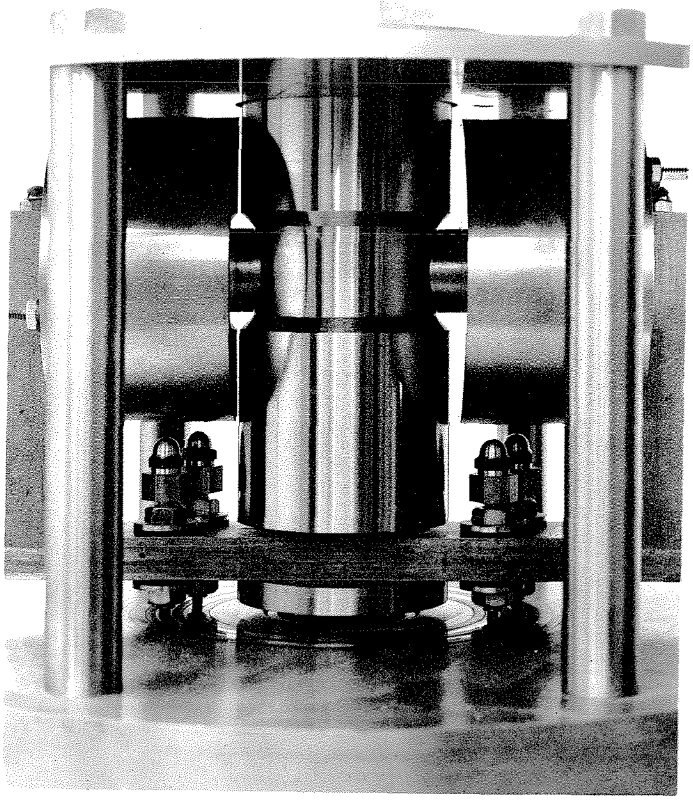

Figure 11A. Electromagnetic Drive

Figure 12A. Impeller and Agitator Drives (original)

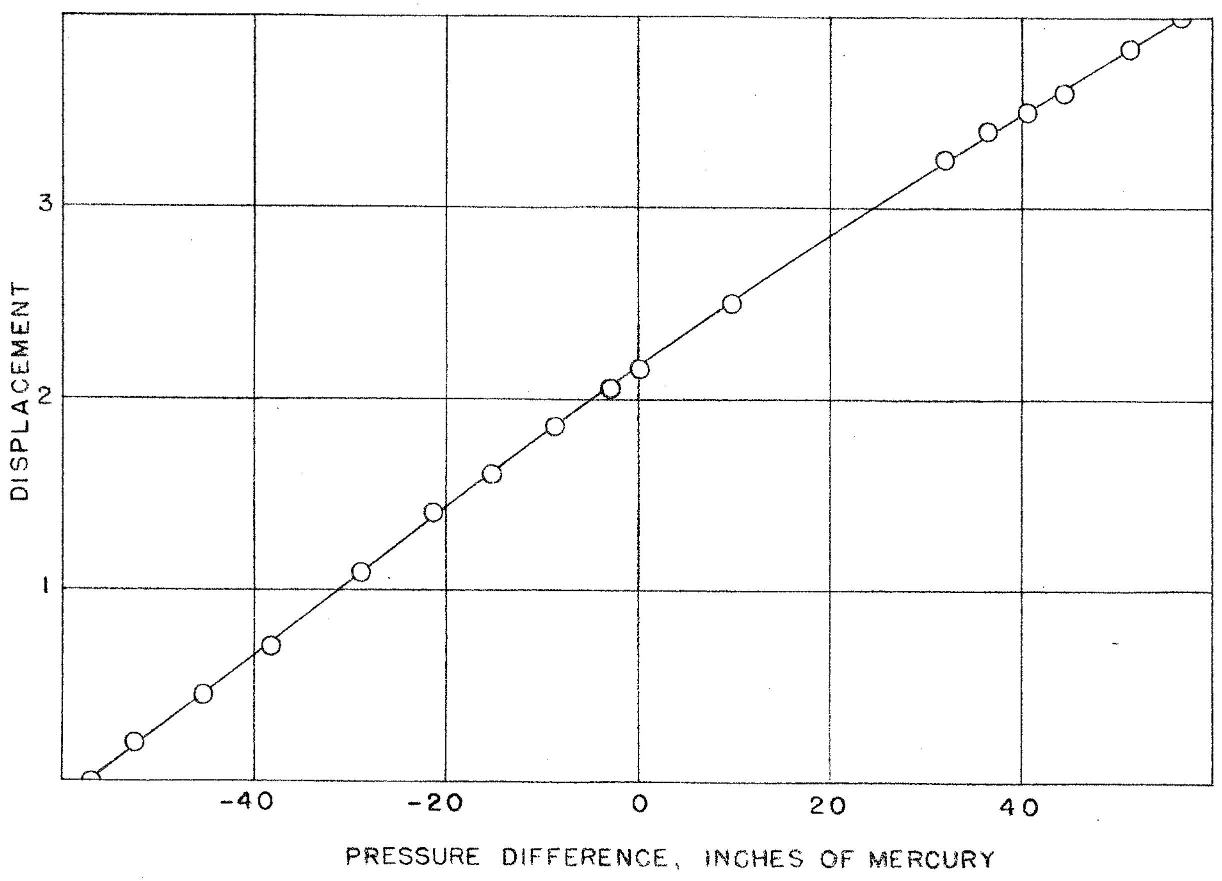

Figure 13A. Displacement Curve, Pressure Diaphragm

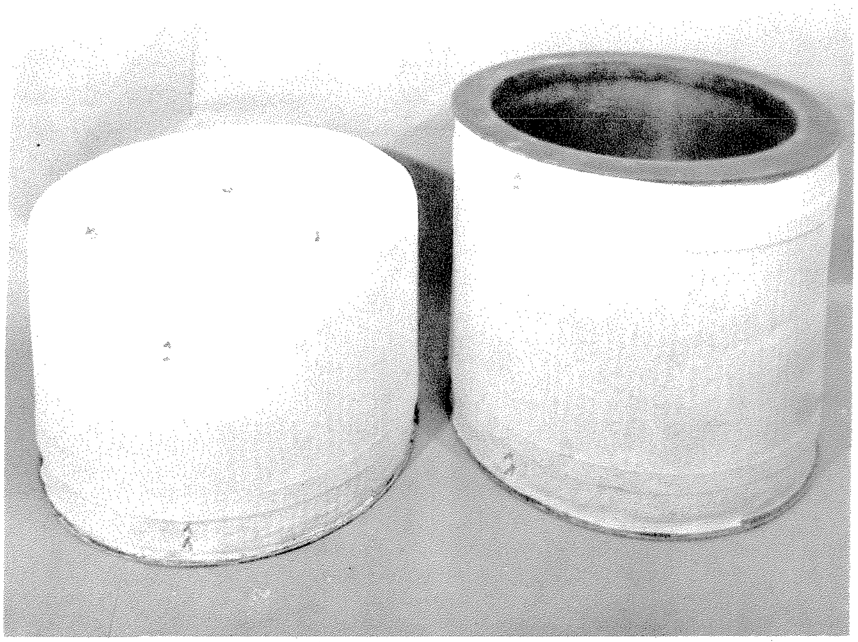

Figure 14A. Adiabatic Jacket

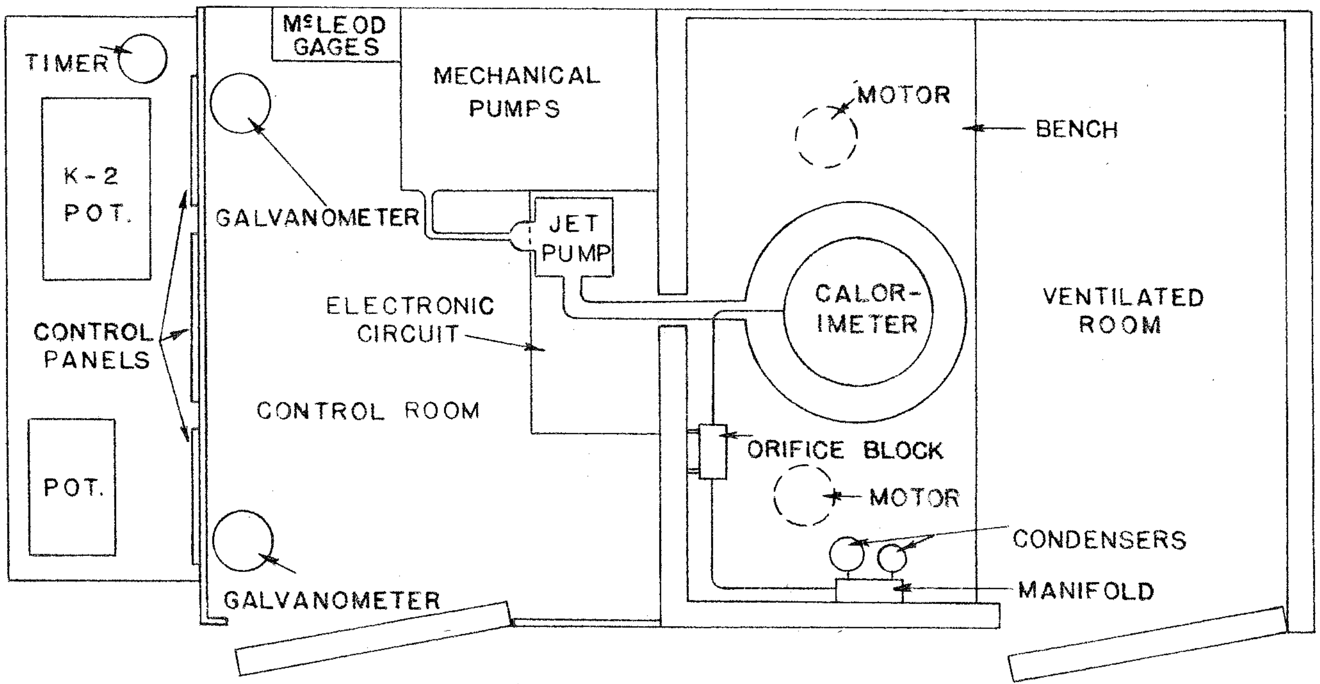

Figure 15A. General Arrangement of Calorimeter and Control Equipment

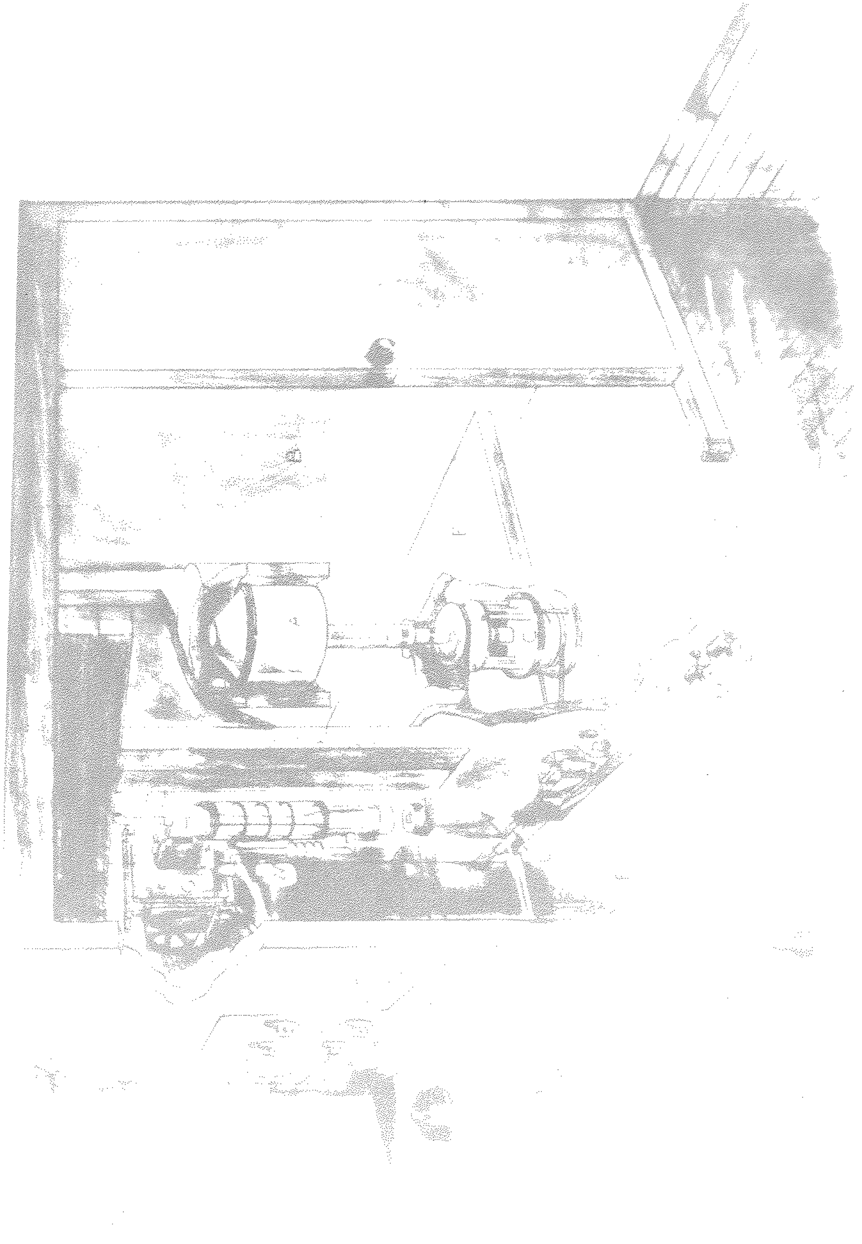

Figure 16A. Calorimeter Housing Unit

LEGEND - FIGURE 16A

A	oil bath
B	calorimeter room
C	drive mechanisms for agitator and impeller
D	adiabatic jacket
E	shelf
F	equipment room
G	mechanical vacuum pump
H	three-stage jet pump
I	L & N Student potentiometer
J	galvanometer
K	photoelectric circuit
L	light source
M	light source
N	mirror in light path from M to O
O	ground glass scale
P	control panel for circuit K
Q	control panel for potentiometer I
R	L & N type K-2 potentiometer
S	controls for calorimeter heater
T	ground glass scale
U	light source
V	mirror in light path from U to T
W	location of vacuum pumps
X	control panel for oil bath heaters

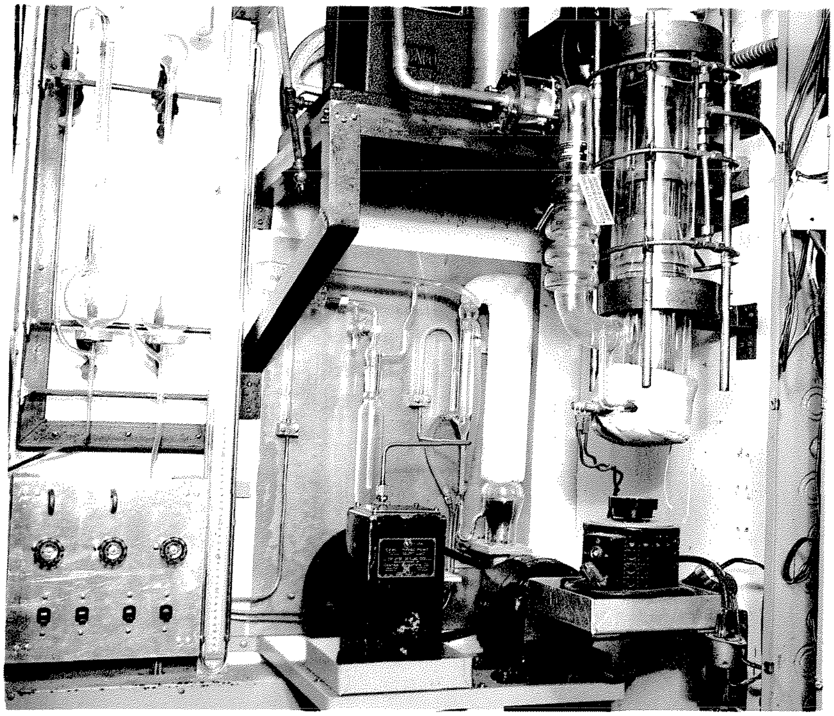

Figure 17A. Vacuum Pumps

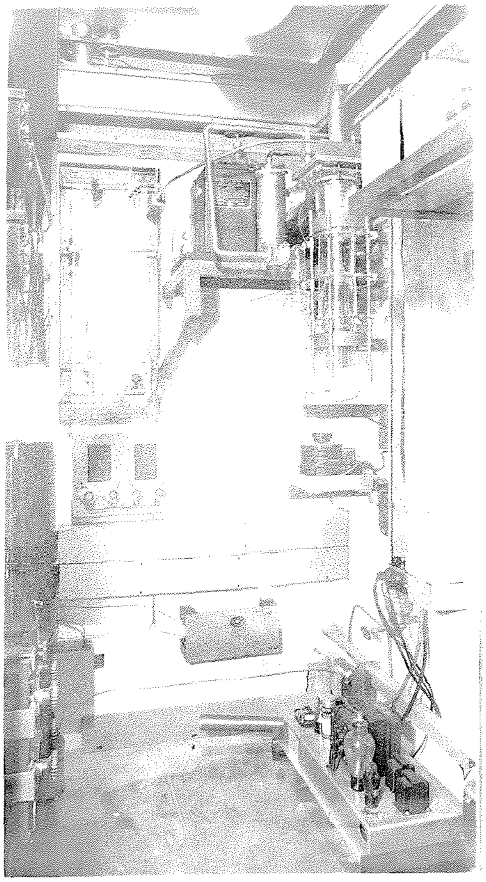

Figure 18A. Interior of Control Room

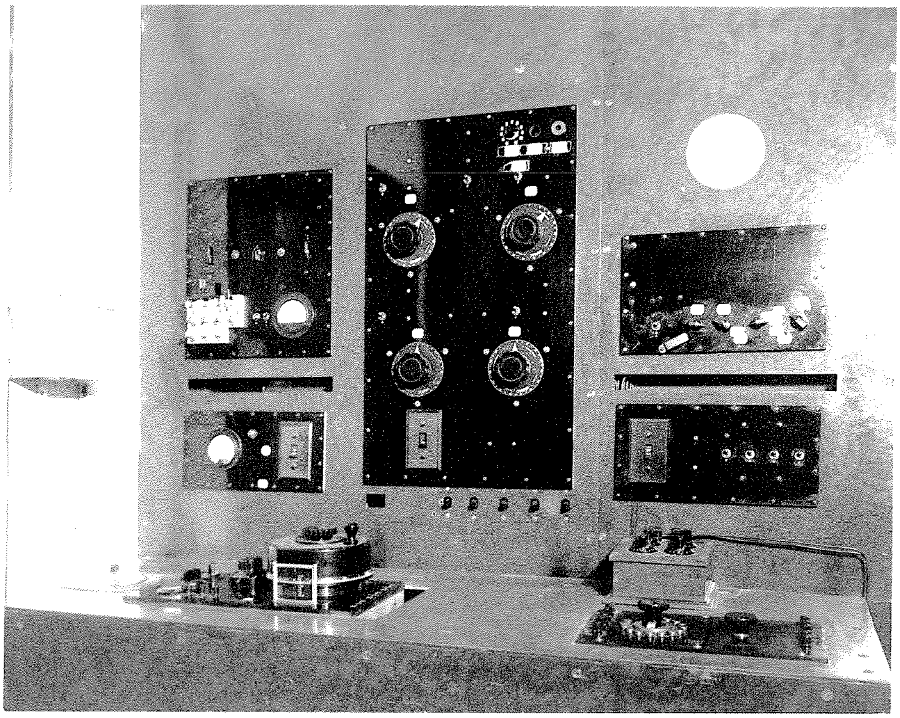

Figure 19A. Control Panels of Figure 16A.

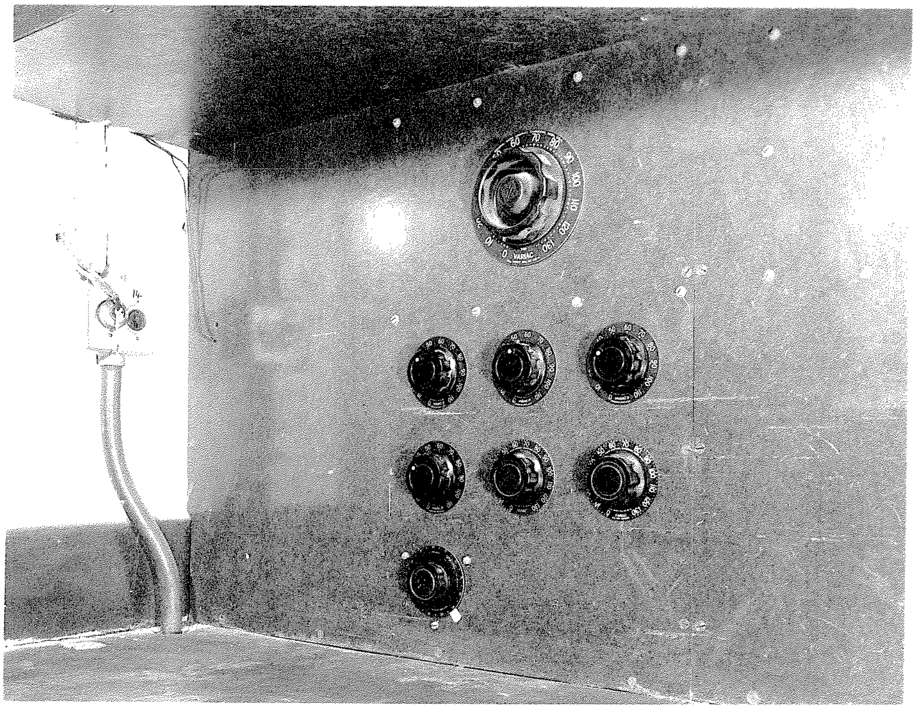

Figure 20A. Control Panel

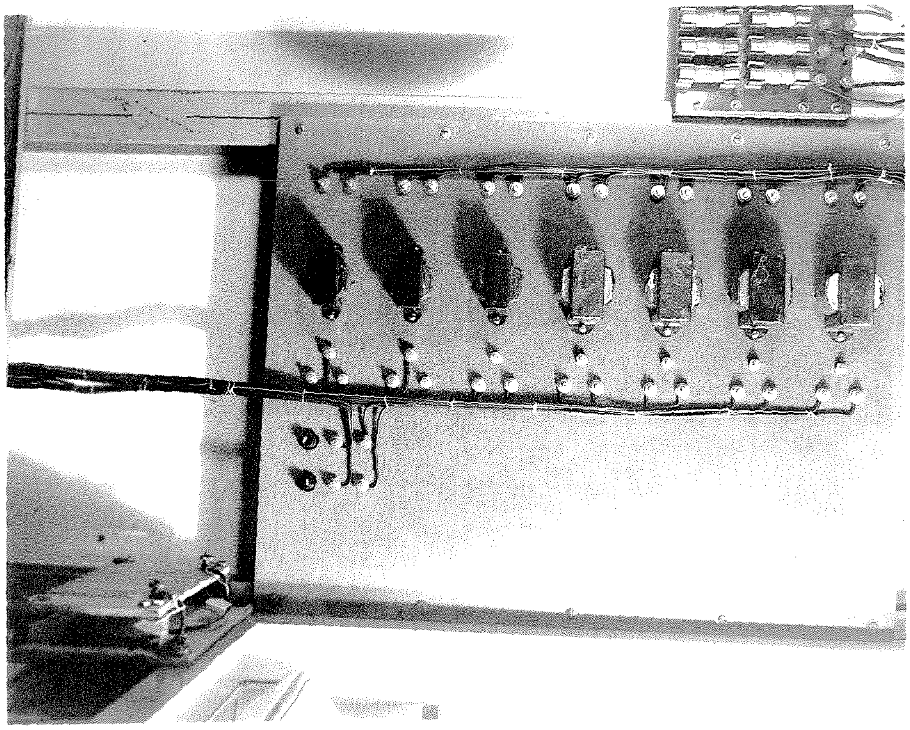

Figure 21A. Transformer Installation

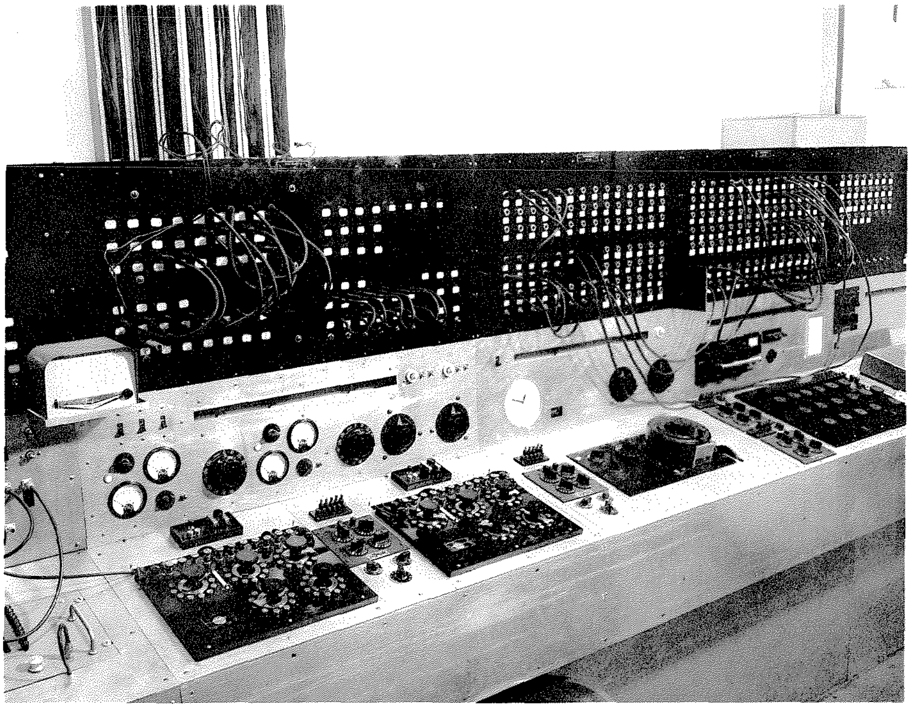

Figure 22A. Controls and Instruments

LIST OF TABLES (APPENDIX)

TABLE IA

Agitator Power[*] vs. Temperature

Temperature °F	Agitator Power watt
100	0.0199
130	0.0195
160	0.0190
190	0.0186
220	0.0182
250	0.0176
280	0.0170
310	0.0165
340	0.0158

[*] Approximately 540 to 610 grams of n-octane in calorimeter

TABLE IIA

Results of Heat Transfer Calibration

Temperature °F	Proportionality Constant k watt sec./ohm sec.
100	1.229
130	1.369
160	1.505
190	1.642
220	1.781
250	1.918
280	2.507
310	2.197
340	2.335

PART II

VOLUMETRIC AND PHASE BEHAVIOR IN THE ETHANE-PROPENE SYSTEM

In the original copy of this thesis the pages indicated above contain the text of a published article:

"Volumetric and Phase Behavior in the Ethane-Propene System"
by R. A. McKay, H. H. Reamer, B. H. Sage,
and W. N. Lacey

Industrial and Engineering Chemistry, vol. 43,
pp. 2112-2117 (1951)

Reprinted from INDUSTRIAL AND ENGINEERING CHEMISTRY, Vol. 43, Page 2112, September 1951

Volumetric and Phase Behavior in the Ethane-Propene System

R. A. McKAY, H. H. REAMER, B. H. SAGE, AND W. N. LACEY
California Institute of Technology, Pasadena 4, Calif.

A knowledge of the volumetric and phase behavior of binary mixtures of ethane and propene is of direct industrial interest in connection with petroleum refining operations.

The molal volume of three mixtures of ethane and propene was measured at pressures up to 10,000 pounds per square inch in the temperature interval between 10° and 400° F. The composition of the coexisting phases was established throughout the two-phase region of this system at temperatures above 10° F.

The data obtained permit interpolation of the volumetric behavior of this binary mixture throughout the stated ranges of pressure and temperature and show satisfactory agreement with earlier volumetric measurements. The deviation from ideal solutions is negative at pressures below 1600 pounds per square inch and positive at higher pressures. However, the magnitude of the positive deviation again decreases at pressures above 2000 pounds per square inch and is relatively small at 8000 pounds per square inch. This decrease serves to confirm earlier trends, which indicate that hydrocarbon mixtures exhibit relatively simple volumetric behavior at high pressures. The equilibrium ratios for the components follow the pattern found for other hydrocarbon systems. The deviation from ideal solutions and from the behavior of these components in other binary systems was significant.

• • • • •

DURING the past few years information about the phase behavior of the ethane-ethene-propene system has come to be of particular industrial interest. The present study relates to the establishment of the volumetric and phase behavior of the ethane-propene system which constitutes a part of the above-mentioned ternary system. The phase behavior of the ethane-propene system was investigated earlier at temperatures from −35° to 200° F. for pressures up to about 750 pounds per square inch (*12*). Volumetric measurements for this system for pressures up to 3250 pounds per square inch in the temperature interval between 212° and 482° F. recently became available (*15*). Disagreement, particularly in regard to the phase behavior of this system, has been found between the earlier measurements of Lu, Newitt, and Ruhemann (*12*) and the present data.

PROPOSITIONS

1. The direct determination of latent heat of vaporization experimentally involves a non-equilibrium evaporation with superheating of the liquid. The exact temperature at which evaporation takes place is not measured. In regions where such direct determinations are feasible, the temperature of the liquid or of the gas may be taken as the temperature of vaporization with very small error.

2. Procedures (1,2) used in this laboratory for measuring the heat capacity of liquids included a heating period followed by a "conditioning" period of the same duration for the attainment of thermal equilibrium. It should be possible to save nearly 40 per cent of the time required for the associated measurements by shortening the conditioning periods.

3. Orifice plates with small holes of controlled size (< 0.002 inch) may be made by plating to size larger holes which can be produced easily.

4. The electroplating of chromium from chromic acid solutions directly onto cast iron or chilled iron is often unsatisfactory with respect to uniformity and adhesion. It is suggested that these difficulties are associated with the presence of graphite in the base metal. The problem might be resolved through a study of the hydrogen overvoltage on

a graphite cathode as a function of concentration and current density in chromic acid solutions.

5. Tinned contacts amalgamated with mercury would provide instrument switches offering low contact resistance with low pressure contact.

6. By comparing the speed of rotation of the front and rear wheels, and assuming adequate power or adequate brakes, a feedback control system might be used to optimize acceleration or deceleration of an automobile. Such a system could assist racing drivers as well as drivers interested in avoiding skids in case of sudden stops.

7. The AEC has encountered difficulty in sampling very fine dust in air. The condensation of liquids on the dust particles could increase the particle size sufficiently to permit removal by filtration. High-boiling liquids whose vapors supersaturate would be preferred for this application.

8. Acetylene has been manufactured by the thermal cracking of hydrocarbons in a regenerative furnace. Wulff (3) presented the basic ideas of the furnace which was developed by Coberly (4) and Hasche (5). During the heating cycle, fuel is fed centrally to a combustion chamber. The combustion chamber increases the steam required to purge the furnace prior to cracking and interferes with the control of the

residence time in the cracking zone. The elimination of the combustion chamber is proposed.

9. a) Refrigeration-type air conditioners for household use provide cooling with little or no independent control of humidity. The result is that the cooled air is often either too humid or too cold for comfort. The incorporation of a counter-current heat exchanger between the air streams to and from the cooling coils would alleviate this difficulty.

b) Air coolers of the evaporative type provide the desired cooling at the expense of the humidity. A scheme is proposed wherein ambient air is cooled in passing into a building through half of a rotating heat exchanger. The exchanger in turn is cooled by air passing from the building and through an evaporative cooler before entering the other half of the exchanger.

10. a) In the repairing of damaged skulls, plates of metal or plastic, and networks of bone fragments taken from the damaged skull have been used. The chief disadvantage in the use of bone fragments lies in the difficulty in supporting the fragments until the network becomes rigid through normal healing processes. A technique is proposed whereby temporary support is given by reducing the atmospheric pressure on the scalp. Under the influence of the resulting pressure difference, the dura mater moves outward against

the network, thus acting as a molding surface for support.

b) The design is proposed for a vacuum regulator which gives regulation of approximately ± 0.5 mm over the range 0 to 20 cm of mercury.

References

(1) Stewart, Jr., R. M., Calorimeter No. 1, Student Report No. 348, Department of Chemical Engineering, California Institute of Technology, 1950.

(2) Sage, B. H. and Hough, E. W., Calorimeter for Some Corrosive Liquids. Anal. Chem. 22, 1304 (1950).

(3) Wulff, U.S. 1,834,965 February 9, 1932; U.S. 1,880,307-10 October 4, 1932; U.S. 1,917,672 July 11, 1933; U.S. 2,037,056 April 14, 1936.

(4) Ind. Eng. Chem. 45, 2596 (1953).

(5) Ind. Eng. Chem. 47, 1517 (1955).